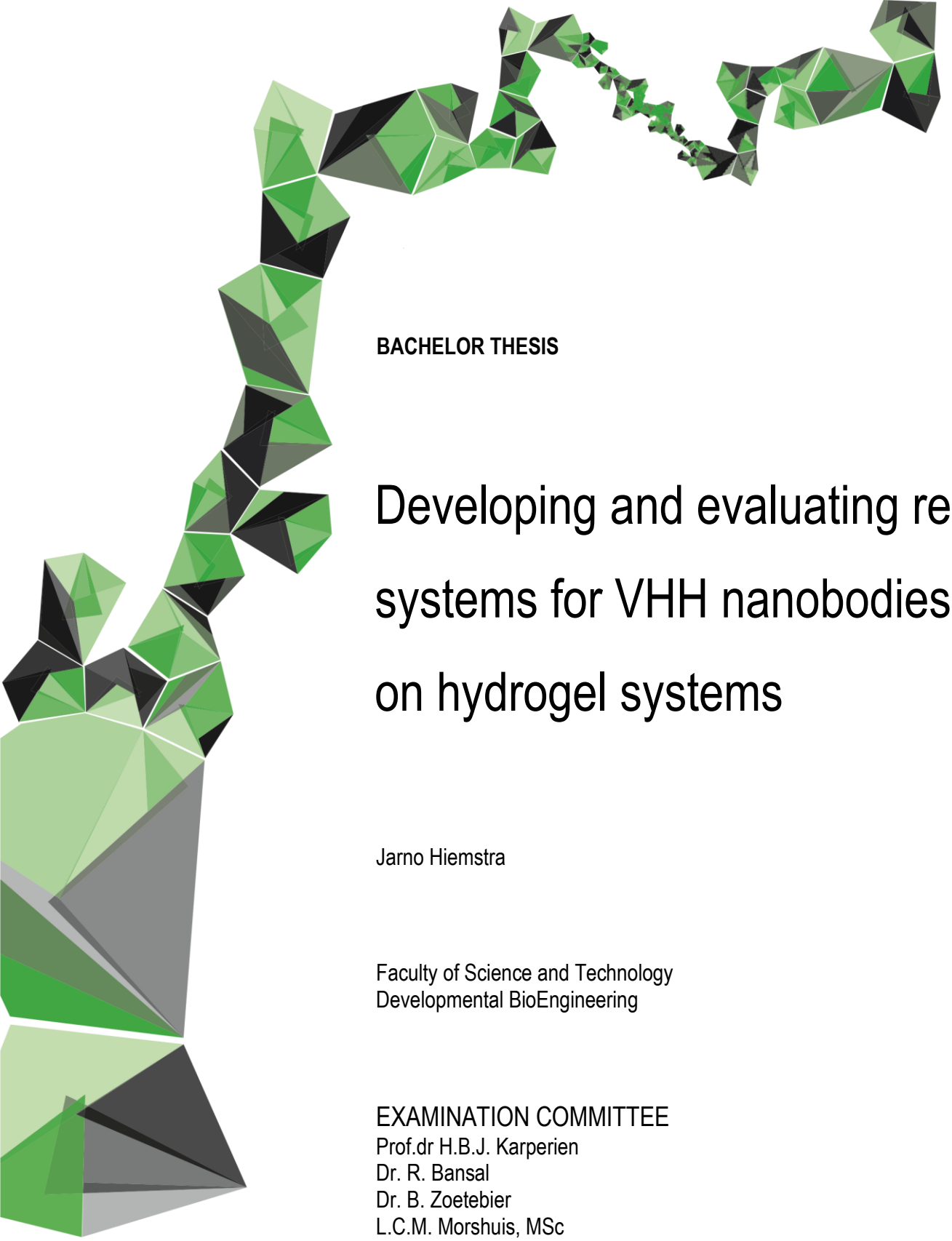

BACHELOR THESIS

Developing and evaluating release systems for VHH nanobodies based on hydrogel systems

Jarno Hiemstra

Faculty of Science and Technology
Developmental BioEngineering

EXAMINATION COMMITTEE
Prof.dr H.B.J. Karperien
Dr. R. Bansal
Dr. B. Zoetebier
L.C.M. Morshuis, MSc

July 7, 2021

UNIVERSITY OF TWENTE.

ABSTRACT

Osteoarthritis (OA) is a chronic joint disease affecting nearly 1.5 million people in the Netherlands only. Currently, there are only treatments available that treat the symptoms of OA and not the disease itself. Variable domain of the heavy chain only antibodies (VHHs) can potentially play a role in the treatment of OA. Due to the low retention time of these VHHs in the body, it is beneficial to use an injectable hydrogel as release system for these VHHs. In this research the effect of electrostatic interactions between the VHHs and the polymers on the release profiles of three types of VHHs from multiple hydrogels was evaluated.

The release profiles were obtained by measuring the fluorescence intensity of released VHHs that were labelled with a FITC-NHS dye over a time frame of 10 days. The fluorescence intensity of the hydrogels themselves was also determined over a time frame of 10 days. The release profiles of Dextran-Tyramine (Dex-TA) based hydrogels with Gelatin-Tyramine (positively charged) or Heparin-Tyramine (negatively charged) added to them clearly showed the influence of electrostatic interactions between the polymer backbone and the incorporated VHHs. Hyaluronic Acid-Tyramine (HA-TA) and Chondroitin Sulfate-Tyramine (CS-TA) hydrogels did not show a clear influence of electrostatic interactions on the VHH release.

Furthermore, the presence of VHHs in collected PBS samples and the binding specificity of the VHHs after release from the hydrogels were assessed with an ELISA assay. The results of the ELISA assay to determine the presence of VHHs in the collected PBS samples showed clear similarities with the fluorescence intensity measurements of the Dex-TA based hydrogels. These similarities were not visible in the measurements of the HA-TA and CS-TA hydrogels. For all types of hydrogel VHH presence in the collected PBS samples was confirmed. Regarding the binding specificity of the VHHs after release, it can be concluded that there was an almost complete loss of binding affinity to the VHH targets. However, further research is necessary to confirm or refute these findings.

Finally, the interactions between cartilage tissue and the VHHs were studied by monitoring these interactions over time in two experiments. These experiments showed that the VHHs interacted with the cartilage tissue, but the exact mechanism of this interaction could not be determined.

In conclusion, Dex-TA based hydrogels show great potential as release systems for VHH nanobodies, since it seems that the VHH release from this type of hydrogel can easily be tuned by varying the polymer charge.

SAMENVATTING

Osteoartrose (OA) is een chronische gewrichtsaandoening die enkel in Nederland al bijna 1.5 miljoen mensen treft. Momenteel zijn er alleen behandelingen beschikbaar die de symptomen van OA behandelen en niet de aandoening zelf. Variabel domein van de zware keten antilichamen (VHH's) kunnen potentieel een rol spelen in de behandeling van OA. Vanwege de lage retentietijd van de VHH's in het lichaam, is het gunstig om een injecteerbare hydrogel te gebruiken als afgiftesysteem voor deze VHH's. In dit onderzoek is het effect van elektrostatische interacties tussen de VHH's en de polymeren op de afgifteprofielen van drie VHH types uit meerdere hydrogels beoordeeld.

De afgifteprofielen werden verkregen door de fluorescentie intensiteit van de afgegeven VHH's, die gelabeld waren met een FITC-NHS fluorofoor te meten gedurende een tijdsbestek van 10 dagen. De fluorescentie intensiteit van de hydrogels zelf werd ook bepaald gedurende een tijdsbestek van 10 dagen. De afgifteprofielen van op Dextran-Tyramine (Dex-TA) gebaseerde hydrogels, waaraan Gelatine-Tyramine (positief geladen) of Heparine-Tyramine (negatief geladen) was toegevoegd, lieten duidelijk de invloed van elektrostatische interacties tussen de polymeren en de toegevoegde VHH's zien. Hyaluronzuur-Tyramine (HA-TA) en Chondroïtinesulfaat (CS-TA) hydrogels lieten geen duidelijke invloed zien van elektrostatische interacties op de VHH afgifte.

Daarnaast werden de aanwezigheid van VHH's in verzamelde PBS-monsters en de bindingsspecificiteit van de VHH's na afgifte uit de hydrogels bepaald door middel van een ELISA assay. De resultaten van de ELISA assay om de aanwezigheid van VHH's in de verzamelde PBS-monsters te bepalen lieten duidelijke overeenkomsten zien met de metingen van de fluorescentie intensiteit van de op Dex-TA gebaseerde hydrogels. Deze overeenkomsten waren niet zichtbaar bij de HA-TA en CS-TA hydrogels. Voor alle typen hydrogels werd de aanwezigheid van VHH's in de verzamelde PBS-monsters aangetoond. Met betrekking tot de bindingsspecificiteit van de VHH's na afgifte, kan worden geconcludeerd dat de bindingsaffiniteit van de VHH's voor het antigeen bijna volledig verdwenen was. Verder onderzoek is echter nodig om deze bevindingen te bevestigen of te weerleggen.

Tot slot zijn de interacties tussen kraakbeenweefsel en de VHH's onderzocht door de interacties over tijd te monitoren in twee experimenten. Deze experimenten lieten zien dat de VHH's een interactie hadden met het kraakbeenweefsel, maar de exacte mechanismes van deze interactie konden niet worden bepaald.

Concluderend, op Dex-TA gebaseerde hydrogels laten veel potentie zien als afgiftesystemen voor VHH nanolichamen, aangezien het erop lijkt dat de VHH afgifte vanuit deze hydrogels gemakkelijk kan worden aangepast door het variëren van de polymeerlading.

CONTENTS

1 INTRODUCTION

1.1 Osteoarthritis

Articular cartilage is a type of tissue known for its poor self-renewal ability [1]. This is due to the avascular nature of articular cartilage and the limited amount of chondrocytes present in the articular cartilage. The migratory ability of these chondrocytes is limited, which also contributes to the poor self-renewal ability of the articular cartilage [2].

In osteoarthritis (OA), articular cartilage degradation, formation of osteophytes, subchondral sclerosis and synovial hyperplasia occur [3]. In the Netherlands only, this chronic joint disease affects almost 1.5 million people, of which nearly half of the patients are diagnosed with OA of the knee [4]. There are multiple suspected risk factors for OA: age, gender, obesity, genetics and diet [5]. As shown in figure 1.1, the prevalence of OA increases rapidly from the age of 50 [4]. The suspected mechanisms that cause OA probably involve weakening of the muscles, cartilage thinning and oxidative damage [5]. However, the exact mechanism is still not fully known. Furthermore, figure 1.1 shows that the prevalence of OA is significantly higher in women than in men. The reason for this phenomenon is also poorly understood at this moment [5].

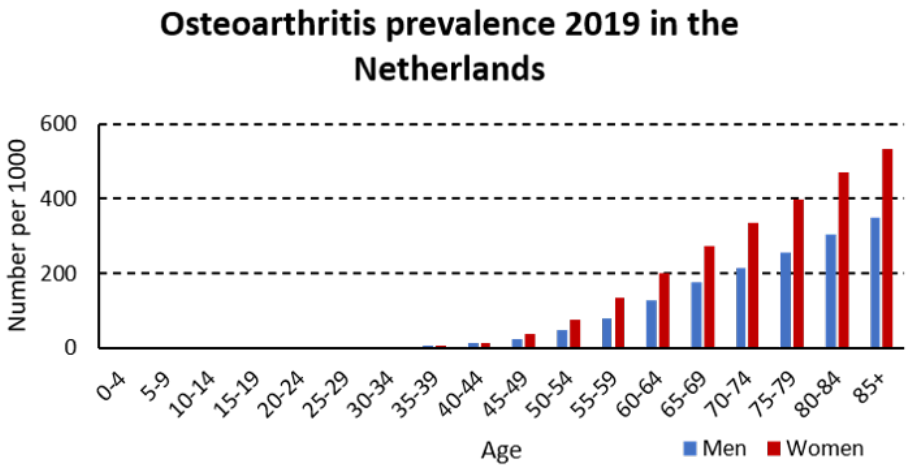

Figure 1.1: An overview of the prevalence of OA against the age of both men and woman, which shows an upwards trend with increasing age. It also shows that the prevalence of OA is higher in women for every age group [4].

The traditional treatment for OA consists of pain management and eventually replacing the joint when the disease is in an advanced stage [6]. These treatments are not ideal, since they only treat the symptoms and not the disease itself. So at the moment there is no effective treatment for OA.

Currently, research is performed on targeting pathological mechanisms of OA with monoclonal antibodies and in some cases this shows great potential [7]. Figure 1.2 shows an overview of different monoclonal antibodies targeting these mechanisms, which all have a significant impact on symptoms involved in OA. One of the downsides of using monoclonal antibodies, however, is their inability to penetrate deep into tissues [8].

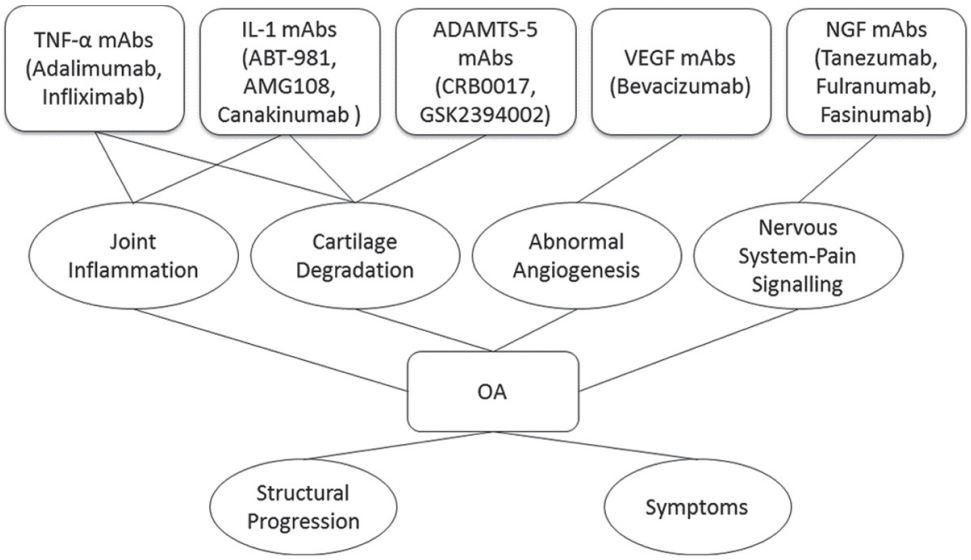

ADAMTS: A Disintegrin And Metalloproteinase with Thrombospondin motifs

TNF: Anti-Tumour Necrosis Factor;

IL-1: Interlerukin-1;

NGF: Nerve growth factor;

OA: Osteoarthritis;

VEGF: Vascular Endothelial Growth Factor (VEGF)

mAbs: Monoclonal Antibodies;

Figure 1.2: An overview describing different mechanisms involved in the pathogenesis of OA with the corresponding monoclonal antibody targets. These mechanisms seem promising to target for a potential OA antibody treatment. [7].

1.2 VHH nanobodies

Variable heavy domain of the heavy chain only antibodies (VHHs) can play a role in a possible treatment for OA.[9]. These VHHs are obtained from the heavy chain only antibodies of camelids. Heavy chain only antibodies logically lack the light chains and furthermore they lack the C_H1 domain in the heavy chain, as shown in figure 1.3. Therefore these heavy chain only antibodies have a molecular weight of 95 kDa compared to 150 kDa in monoclonal antibodies. The antigen binding domain of the heavy chain only antibody is the VHH nanobody, which has a molecular weight between 12 and 14 kDa [8]. Next to their small size, other important properties of VHH nanobodies are their high solubility, stability, specificity and affinity. The high solubility is a result of a substitution of four hydrophobic amino acids (V42, G49, L50 and W52) in the variable heavy domain of a human antibody by five hydrophilic amino acids (F42 or Y42, E49, R50 and G52) in the VHHs of camelids [8]. The high stability is obtained because of an extra disulphide bond between CDR1 or CDR2, and CDR3, for respectively camelid and llama VHHs. Cloning VHHs is also a relatively easy process to perform and they have good thermal and chemical resistance [10]. In addition, the human variable heavy domain and the VHH amino acid sequence are for approximately 80 percent identical. Therefore VHH nanobodies have low immunogenicity and can be administered in the human body rather safely [8, 11].

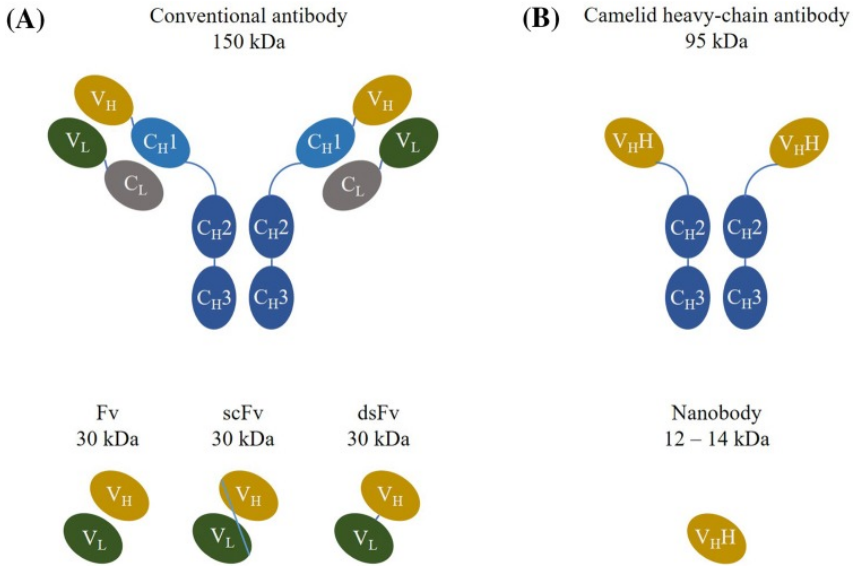

Figure 1.3: A comparison between a conventional antibody (A) and a camelid heavy chain antibody (B), which shows that the heavy chain antibody lacks the light chain and the C_H1 domain compared to the conventional antibody. Furthermore, the VHH nanobody which can be obtained from the heavy chain antibody, is shown in the bottom right of the image [8].

Currently, research is being done on using VHHs for therapeutic purposes. These researches concern for example the treatment of tumors, and also in tissue engineering VHHs show great potential. The main reason for this is the fact that conventional antibodies have limited tissue penetration because of their relatively high molecular weight of 150 kDa. VHHs on the other hand have a molecular weight of 12 to 14 kDa. Because of this difference in molecular weight, VHHs have much better tissue penetration, which makes that they can be of great use in the treatment of OA [8]. However, this low molecular weight of the VHHs can also be a disadvantage. The half-life time of the VHHs in tissue will only be a few hours, since a molecular weight lower than 50-60 kDa leads to glomerular filtration [8, 10]. Combining the VHHs with a hydrogel based release system could be a possible solution for this problem.

1.2.1 VHH selection

In this research three VHHs with different targets that have a role in the OA pathogenesis have been selected, mainly based on their isoelectric point. This way, a positively ,neutrally and negatively charged VHH could be obtained when studied in a PBS solution with a neutral pH. This is desirable to study the effect of electrostatic interactions between a polymer and a VHH on the release of these VHHs from a hydrogel. In the following section the role of each of the targets of the selected VHHs in the OA pathogenesis is briefly explained, as well as the isoelectric point of the respective VHH.

1.2.1.1 Matrix metalloproteinase 9

Matrix metalloproteinases (MMPs) are heavily involved in the OA pathogenesis [12]. The main MMPs known to be involved are MMP-1, MMP-3 and MMP-13, which all induce the degradation of cartilage. Lately, the role of MMP-9 has been investigated as well and research has shown that the MMP-9 protein levels were increased in OA patients [13]. Furthermore, MMP-9 is involved in the activation of other MMPs and cytokines [14]. For example, a positive correlation between MMP-9 and MMP-13 expression has been found in OA [15]. It was also suggested that MMP-9 is involved in the vascular invasion during OA [14]. In conclusion, there is still a lot unknown about the possible involvement of MMP-9 in OA, but there are multiple signals that it plays a role in OA pathogenesis. Therefore it can potentially be an important target for OA treatment.
The VHH against MMP-9 has a PI value of 8.7, which makes it a positively charged VHH when dissolved in PBS with a neutral pH.

1.2.1.2 Tropomyosin receptor kinase A

Tropomyosin receptor kinase A (TrkA) is another potential target for the treatment of OA. This receptor has a high affinity for binding Nerve Growth Factor (NGF), which is known to induce hyperalgesia [16, 17]. This pain hypersensitivity is the result of endocytosis of the NGF-TrkA complex in neuronal cell bodies, where the complex has an influence on multiple receptors and ion channels. This can eventually cause pain hypersensitivity [18].
The use of anti-NGF monoclonal antibodies has already shown pain reduction in OA, however, adverse events are still a problem at the moment[19, 20]. Therefore anti-TrkA VHHs might serve as a promising alternative for the treatment of pain hypersensitivity in OA.
The VHH against TrkA has a PI value of 7.3, which makes it an almost neutrally charged VHH when dissolved in PBS with a neutral pH.

1.2.1.3 Tumor necrosis factor alpha

Tumor necrosis factor alpha (TNFα) is an inflammatory cytokine involved in the pathogenesis of OA. It plays a role in the induction of iNOS, COX-2, IL-6 and PGE_2 production. In addition, the production of type II collagen, proteoglycans, and proteoglycan-binding proteins is inhibited by TNFα [21]. It also induces the expression of MMPs, inhibits chondrogenesis and it can induce chondrocyte apoptosis [22]. Furthermore, TNFα is involved in the process of bone remodelling by inducing osteoclastogenesis and inhibiting the differentiation of Mesenchymal Stem Cells into osteoblasts [21].
The VHH against TNFα has a PI value of 5.8, which makes it a negatively charged VHH when dissolved in PBS with a neutral pH.

1.3 Hydrogels

Hydrogels show great potential as drug delivery systems [23]. Compared to freely administered VHHs in the joint, the use of a hydrogel could increase the half-life time significantly [24]. Because of this, VHHs could possibly be administered over a longer period of time by the hydrogel based release system. The hydrogel has to be injectable, since this has a lot of advantages over a conventional preformed hydrogel. Injectable hydrogels are ideal for filling non-uniform defects in cartilage, the procedure is minimally invasive and there is the possibility to incorporate cells or bioactive molecules (VHHs in this research) to the injectable solution [25].

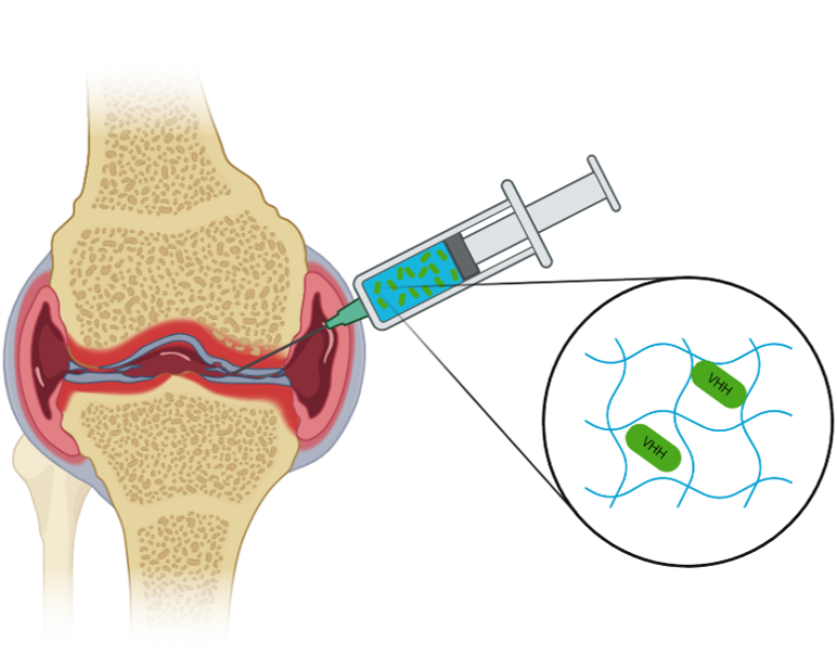

Figure 1.4: A schematic representation of the concept of an injectable hydrogel with VHHs incorporated in this hydrogel.

The hydrogels used in this research will consist of a single polymer backbone or a mixture of one polymer with a small amount of another polymer. Depending on the polymer(s) that form(s) the backbone of the hydrogel, the charge of the hydrogel can vary. This charge will probably have an effect on the release of the VHHs out of the hydrogel. Another factor that could influence the release of the VHHs is the mesh size of the hydrogel. When the mesh size is bigger than the size of the VHH, the VHH release will be mainly based on diffusion, because in this situation the VHHs can move freely through the hydrogel. If the size of the VHHs is close to the mesh size, steric hindrance will lead to slower diffusion rates. When the mesh size is smaller than the VHH size, the VHHs will not be able to migrate through the gel. In this last case degradation, swelling or deformation is necessary to release the VHHs [26]. In this research five different polymer backbones that are functionalized with Tyramine will be used to prepare hydrogels with varying charges: Dextran-Tyramine, Hyaluronic Acid-Tyramine, Chondroitin Sulfate-Tyramine, Dextran/Gelatin-Tyramine (95:5 ratio) and Dextran/Heparin-Tyramine (95:5 ratio). The approximate zeta potentials of the polymers can be found in table 1.1.

Table 1.1: An overview of the approximate zeta potentials of the different polymers used to prepare hydrogels.

Polymer backbone	Zeta potential (mV)
Dextran-Tyramine	Neutral [27]
Hyaluronic Acid-Tyramine	-36 [28]
Chondroitin Sulfate-Tyramine	-49 [28]
Gelatin-Tyramine	+5 [29]
Heparin-Tyramine	-20 [30]

All of these types of hydrogel are injectable, because crosslinking, and hence the gelation process, will only take place after hydrogen peroxide is added to a polymer solution mixed with horseradish peroxidase (HRP) to catalyze the reaction [31]. This reaction is visualized in figure 1.5. Furthermore, these hydrogels all have a gelation time less than 30 seconds, which is desired, since the gel should not leak out after injection into the joint. A gelation time of approximately 20 seconds is ideal if the hydrogel should function as an injectable hydrogel [25]. In addition, the polymers used to prepare these hydrogels all show good biocompatibility, which makes them suitable to administer in the human body [32, 33, 34, 35].

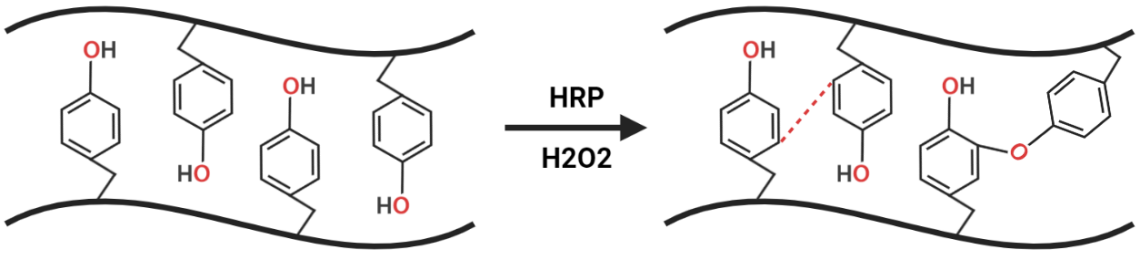

Figure 1.5: An overview of the reaction to crosslink the phenol groups on the polymer backbone by using horseradish peroxidase to catalyze a reaction with hydrogen peroxide.

1.4 Aim of this research

As explained above, incorporating VHHs in hydrogel based release systems seems quite promising for OA treatment. Therefore this research will focus on developing release systems based on different polymer hydrogels with varying charges and evaluating the release profiles of multiple VHHs in these release systems. The VHHs that will be used all have different isoelectric points, which can lead to varying release profiles in the hydrogels, because of possible electrostatic interactions between the polymer backbone and the incorporated VHHs. To evaluate the developed release systems the VHHs will be labelled with a fluorescent label. This ensures that the incorporation of the VHHs in the hydrogel can be analyzed and that the release of the VHHs can be monitored by measuring the fluorescence intensity of the hydrogels and the supernatant. This way, the release profile of each of the VHHs can be determined for the different hydrogels. In addition, the binding specificity after release from the hydrogels will be measured at multiple points in time. To gain more insight into the behavior of VHHs near cartilage tissue, fluorescence microscopy will be used with unprocessed and processed cartilage samples.

1.5 Hypothesis

For this research the hypothesis is made that the negatively charged hydrogels (Dextran/Heparin-Tyramine, Chondroitin Sulfate-Tyramine and Hyaluronic Acid-Tyramine), will hardly release any of the positive VHHs, while the more neutral VHHs will show gradual release from the hydrogel and the negative VHHs will be released very quickly.
The almost neutrally charged hydrogel Dextran-Tyramine, will probably show gradual release of all of the VHHs, since there will be almost no electrostatic interactions between the VHHs and the hydrogels.
Positively charged Dextran/Gelatin-Tyramine is hypothesized to release the neutral VHHs gradually, while the positive VHHs will release very quickly and the negatively charged VHHs will hardly release from the hydrogel.

2 METHODS

2.1 Materials

Five different polymer backbones were used in this research: Dextran-Tyramine (Dex-TA), Dextran/Gelatin-Tyramine (Dex/Gel-TA), Dextran/Heparin-Tyramine (Dex/Hep-TA), Hyaluronic Acid-Tyramine (HA-TA) and Chondroitin Sulphate-Tyramine (CS-TA). Dextran 40EP was obtained from Pharmacosmos, gelatin from Sigma-Aldrich, heparin from Merck, hyaluronic acid from Contipro and chondroitin sulfate from TCI. Dextran was functionalized according to previous protocols described in [36] and HA-TA, CS-TA, Hep-TA en Gel-TA were synthesized by adapting the protocol of HA-TA from [36]. Horseradish peroxidase (HRP) was purchased from Sigma-Aldrich and hydrogen peroxide from Supelco. Phosphate buffered saline (PBS) was purchased from Lonza. Anti-MMP9 VHH, anti-TNFα VHH and anti-TrkA VHH were purchased from QvQ. Fluorescein isothiocyanate-N-Hydroxysuccinimide (FITC-NHS) dye was obtained from Thermo Scientific.

2.2 Fluorescent labelling of the VHHs

To make sure the release profiles of the VHHs from the hydrogels could be monitored, the VHHs were fluorescently labelled. First of all, compared to the VHHs a 10 times molar excess of FITC-NHS dye was added to them. After this, the sample was incubated for 2 hours at room temperature (RT). All unreacted dye in the VHH samples was washed out with 200 µL PBS in 3.5 kDa spin columns. 11 rounds of centrifugation in fresh PBS were used for this process at 14000 rpm and 4°Celsius for 20 minutes. The filtrate was collected and with the VICTOR3 Multilabel Plate Reader (Perkin Elmer) it was checked whether there was any free dye left in the samples. To analyze the VHH concentration in the final sample, first of all the Nanodrop (Thermo Scientific) was used. Besides, a BCA assay was performed with the Pierce BCA Protein Assay Kit (Thermo Scientific, 23225) to determine the VHH concentration. In this assay, the absorbance of unlabelled and labelled VHH against MMP9, TNFα and TrkA was measured at 562 nm in a 96-well plate. To create a calibration curve, the absorbance of Bovine Serum Albumin (BSA) was measured for a range from 2000 to 0 µg/mL and with this calibration curve the concentrations of the samples were determined. Since the concentrations of the unlabelled VHHs were already known, these concentrations were used to scale the measured values.

2.3 Hydrogel formation

In this research five different polymer backbones were used to prepare hydrogel based release systems for VHHs: Dextran-Tyramine (Dex-TA), Dextran/Gelatin-Tyramine (Dex/Gel-TA), Dextran/Heparin-Tyramine (Dex/Hep-TA), Hyaluronic Acid–Tyramine (HA-TA) and Chondroitin Sulphate-Tyramine (CS-TA). In the case of Dex/Gel-TA and Dex/Hep-TA these polymers were mixed in a 95:5 ratio respectively.

For all polymers, 10% w/v hydrogel was prepared by making a 12.5% polymer stock solution in PBS. To each of the polymer solutions the correct amount of VHH was added to obtain a 5, 10 or 15 µg/mL concentration. Furthermore, a 30 u/mL stock solution HRP was prepared and a 30% stock solution hydrogen peroxide was diluted to a 0.3% solution. These three components were mixed in the following order with the following proportions to prepare a 10% hydrogel: 80% v/v polymer solution, 10% v/v HRP and 10% v/v hydrogen peroxide. The solution was vortexed for four seconds and two 50 µL droplets were pipetted on Parafilm before gelation took place. This resulted in two spherically shaped hydrogels for each of the conditions, that were all placed in a black 96-well plate filled with 150 µL PBS per well.

2.4 VHH release profile measurements

Over a time frame of 10 days, the PBS in the 96-well plate was renewed every day and the old PBS was transferred to a new 96-well plate. This new plate was analyzed with the VICTOR3 Multilabel Plate Reader to monitor the amount of released VHHs from the hydrogels over time. The fluorescence intensity of the hydrogel itself was also analyzed immediately after fresh PBS was added to the wells with the hydrogels. This way the amount of released VHHs and the amount of VHHs that were still incorporated in the hydrogel could both be determined.

2.5 VHH presence in release samples

Next to the fluorescence intensity measurements, an ELISA assay was performed to measure the VHHs themselves. For this assay, the PBS samples that were collected from the release profile measurements on day 1, 4, 7 and 10 were used. A 96-well Maxisorp plate (Thermo Scientific, 44-2404-21) was coated with 50 µL of each of the collected PBS samples and incubated overnight at 4° Celsius. After this process the plate was washed three times with 0.5% PBS-Tween20. 200 µL of 4% Marvel solution in PBS was added to the wells to block all unspecific binding to the plate. The plate was incubated for 1 hour at RT while shaking at 250 rpm, after which the Marvel solution was removed. After three rounds of washing with 0.5% PBS-Tween20, 50 µL of 2000 times diluted goat α-llama IgG (Invitrogen, A16060) in 1% Marvel/PBS was added to each well and incubated for 1 hour at RT while shaking at 250 rpm. Subsequently, the wells were washed three times with 0.5% PBS-Tween20 followed by three times washing with PBS. After this, 100 µL of the color reagent mixture that was was prepared 10 minutes in advance was added to each of the wells. In this mixture color reagent A and B (RnD systems) were mixed in equal volumes. After 20 minutes of incubation at RT while protected from light, the stop solution (N2 H2SO4, RnD systems) was added to the wells. Finally, the absorbance was measured at 450 nm and 650 nm with the Multiskan GO (Thermo Scientific).

2.6 Binding specificity of the VHHs

The binding specificity of the VHHs to their target was also assessed with an ELISA assay. A 96-well Maxisorp plate was coated with 50 µL of 3 µg/mL of human MMP-9 (SinoBiological, 10327-HNAH), human TrkA (SinoBiological, 11073-H08H) and human TNFα (Biolegend, 570104) in sterile PBS and incubated overnight at 4° Celsius. After this process the plate was washed three times with 0.5% PBS-Tween20. 200 µL of 4% Marvel solution in PBS was added to the wells to block all unspecific binding to the plate. The plate was incubated for 1 hour at RT while shaking at 250 rpm, after which the Marvel solution was removed. 50 µL of VHH from the PBS samples collected on day 1, 4, 7 and 10 was added to the wells and the plate was incubated for 1 hour at RT while shaking at 250 rpm. After three rounds of washing with 0.5% PBS-Tween20, 50 µL of 2000 times diluted goat α-llama IgG in 1% Marvel/PBS was added to each well and

incubated for 1 hour at RT while shaking at 250 rpm. Subsequently, the wells were washed three times with 0.5% PBS-Tween20 followed by three times washing with PBS. After this, 100 µL of the color reagent mixture that was was prepared 10 minutes in advance was added to each of the wells. In this mixture color reagent A and B were mixed in equal volumes. After 20 minutes of incubation at RT while protected from light, the stop solution was added to the wells. Finally, the absorbance was measured at 450 nm and 650 nm with the Multiskan GO.

2.7 VHH interaction with human cartilage

The interaction of the VHHs with human cartilage was assessed by placing cartilage samples into a 96-well plate with 10 µg/mL VHH in PBS added to them. These cartilage samples were obtained from two human donors diagnosed with OA. The samples were imaged with a fluorescence microscope (Invitrogen EVOS) after 0, 2, 4, 8, 24 and 48 hours. After 24 hours the 100 µL PBS in the wells was replaced by 100 µL medium to prevent chondrocyte apoptosis.

Furthermore, a second experiment was carried out to study the interaction of the VHHs with human cartilage. In this experiment cartilage tissues were placed in a 96-well plate with 1 µg/mL VHH added to these tissues in 100 µL chondrocyte medium. In this experiment only anti-MMP9 and anti-TNFα VHHs were added, since there were not enough cartilage samples to also include anti-TrkA VHHs. After 1, 4, 8 and 24 hours the samples with anti-MMP9 VHHs were transferred to an Eppendorf tube and washed with PBS. Subsequently the samples were fixated in 4% paraformaldehyde for 30 minutes at RT and washed three times with 0.1% PBS/Tween20 for 5 minutes. For the samples with anti-TNFα VHHs added this was done after 4 and 24 hours. The samples were incubated in 30% sucrose overnight or until the sample sank to the bottom of the tube. After the incubation, the samples were cryopreserved by placing them in a mold filled with Cryomatrix (Thermo Scientific). Subsequently, the samples were immersed in isopentane for 30 seconds. After this process six sections of 5 µm thickness were made with a cryotome for each of the samples and these sections were placed on microscope slides for later imaging with the fluorescence microscope (EVOS).

3 RESULTS

3.1 Fluorescent labelling of the VHHs

During the fluorescent labelling of the VHHs, the filtrate of each centrifugation round was collected. The fluorescence intensity of each of the filtrates was measured to confirm that almost all unreacted dye was removed from the labelled VHH samples. The graph in appendix A.1 confirms that most of the unreacted dye was removed from the labelled VHH samples during the washing procedure.

To determine the concentration of the labelled VHH samples, absorbance measurements were performed with the Nanodrop. The results of these measurements are shown in appendix A.2. The values in table A.1 are the averages of two measurements for each sample. The stock concentration of the VHHs was divided by the value of the corresponding unlabelled VHH measurement at 280 nm and multiplied by the measured absorbance of the labelled VHH at 280 nm. This resulted in the labelled VHH concentrations in table A.2. For anti-MMP9 and anti-TNFα VHHs the measured values seemed realistic. However, for the anti-TrkA VHH sample the measured absorbance led to a concentration that was higher than theoretically possible, since the added amount of VHH could lead to a maximum concentration of 500 µg/mL.

The concentration of the labelled VHH samples was also measured with a BCA assay due to the deviating results described above. The results of this assay are shown in appendix A.3. The measured absorbances of the unlabelled and labelled VHHs in table A.3 were converted to concentrations with the calibration curve in figure A.2. Since the concentrations of the unlabelled VHHs were already known, the determined concentrations were scaled to match these known concentrations. This resulted in the final concentrations in the last column of table A.3. These results seem realistic for all three types of VHHs. For the anti-MMP9 and anti-TNFα VHHs the concentration determined with the BCA assay was significantly lower compared to the Nanodrop measurements. Therefore it seems plausible that the used concentrations in the first release experiment were actually quite a bit lower than initially anticipated.

Finally, the fluorescence intensity of serially diluted samples of the labelled VHHs was measured. This way, it was confirmed that the labelling with the FITC-NHS dye was successful. The results of these measurements are shown in appendix A.4. As expected, they show a gradual decrease in fluorescence intensity, the more the samples were diluted.

3.2 VHH release profile measurements

In this section the results of the VHH release profile experiments are presented. First of all, the results of the daily collected PBS samples and the fluorescence intensity measurements of the hydrogels themselves are shown for the first experiment. After this, the data obtained in the second experiment is shown in a similar way. The results of the daily collected PBS samples are presented as a cumulative release profile in both experiments.

Since the degree of labelling is unknown for the VHHs, it is not possible to compare the release of different VHHs in the same hydrogel directly in a quantitative way. Therefore the release of each of the VHH types was only compared between different types of hydrogel. Despite the unknown degree of labelling, differences in the trends of the release profiles could still be observed.

3.2.1 Experiment 1

In the first release experiment 5, 10 and 15 µg/mL of anti-MMP9 and anti-TNFα VHHs was added to three types of hydrogel: HA-TA, CS-TA and Dex-TA. Anti-TrkA VHHs were not included in this measurement due to the deviating concentration measurement with the Nanodrop. The Dex-TA hydrogel with anti-MMP9 VHH incorporated did not gelate and therefore this combination is not included in the results of this experiment. The measurements on day 6 were performed with PBS that has been surrounding the gel for 72 hours instead of 24 hours, which is something to take into account.

When comparing the release profiles of anti-MMP9 VHHs between the two types of hydrogel in figure 3.1, it stands out that the release from the HA-TA hydrogel decreases a little after day 1, after which it increases again from day 2 to day 3. For the CS-TA hydrogel the release is at its highest point on day 1, after which the release remains almost the same for the next days.

The overall release of anti-MMP9 VHHs is higher with the CS-TA hydrogel than with the HA-TA hydrogel for the 15 µg/mL concentration. For the 10 µg/mL concentration the overall release is almost the same between the hydrogels and for the 5 µg/mL concentration HA-TA shows a higher overall release, since the CS-TA VHH release is extremely low. Based on the zeta potentials of the two polymers, it was expected that the positively charged anti-MMP9 VHHs would be released more from CS-TA than from HA-TA hydrogels.

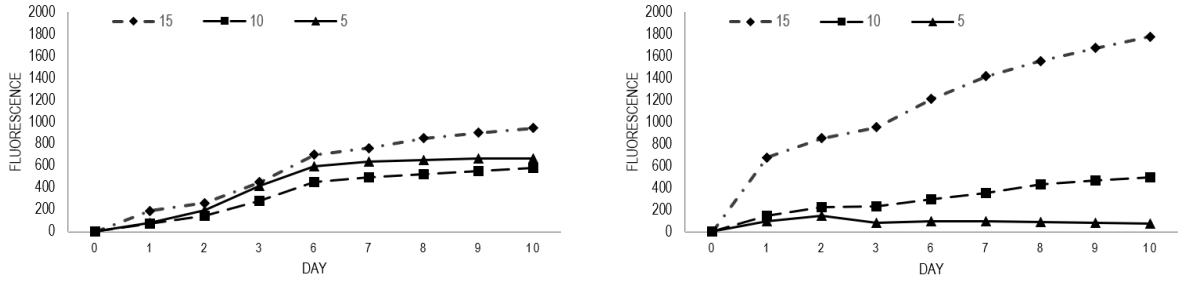

Figure 3.1: The cumulative release of anti-MMP9 VHHs from HA-TA **(a)** and CS-TA **(b)** hydrogels measured over a time frame of 10 days.

When the graphs of the hydrogels with anti-TNFα VHHs incorporated are compared in figure 3.2, it stands out that for the HA-TA and CS-TA hydrogels the 10 µg/mL concentration has a relatively high release compared to the 15 µg/mL concentration. From the HA-TA hydrogel the 10 µg/mL release is even higher than the 15 µg/mL release. In theory the 15 µg/mL concentration should at least have the same release as the 10 µg/mL concentration.

Regarding the release profiles, the daily anti-TNFα VHH release from the HA-TA hydrogel slowly decreases after day 6. With the CS-TA hydrogel there is no clear release profile to be seen, since there are quite some fluctuations in the 15 and 5 µg/mL VHH concentrations. The Dex-TA

hydrogel shows a profile similar to the HA-TA hydrogel. However, in this type of hydrogel no release was measured in the 10 and 5 µg/mL VHH concentration, which is remarkable. The extremely low fluorescence intensity measurements for some of the hydrogels in this experiment could be explained by the fact that the VHH concentrations were measured using the Nanodrop. As explained in section 3.1, the concentrations used in the first release experiment were probably lower than the desired 5, 10 and 15 µg/mL concentrations due to inaccurate Nanodrop measurements.

In terms of overall release the Dex-TA hydrogel shows the highest release for anti-TNFα VHHs, followed by the HA-TA and CS-TA hydrogels. Based on the zeta potentials of the polymers, exactly the opposite was expected for negatively charged anti-TNFα VHHs.

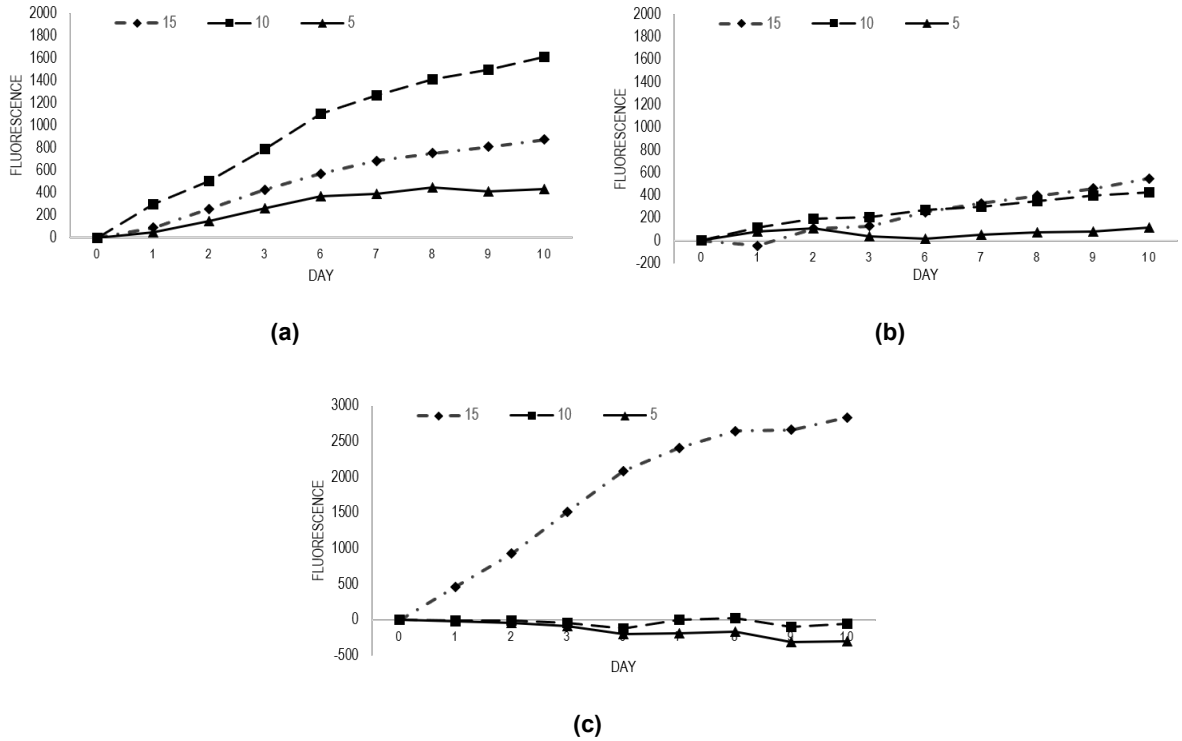

Figure 3.2: The cumulative release of anti-TNFα VHHs from HA-TA **(a)**, CS-TA **(b)** and Dex-TA **(c)** hydrogels measured over a time frame of 10 days.

The results of the fluorescence intensity measurements of the hydrogels themselves are shown in appendix A.5. These measurements were not performed on day 1 and 2. Therefore these results could only be presented as absolute values instead of percentages relative to the fluorescence intensity at day 1. For all of the conditions the measured values show many fluctuations. The fluorescence intensity measurements of the HA-TA hydrogel with anti-MMP9 VHHs incorporated even show negative values. Since it is theoretically not possible to have fluctuations and negative values in these measurements, these results were considered as inaccurate.

3.2.2 Experiment 2

In the second release experiment, only a 15 µg/mL VHH concentration was used in the hydrogels. This concentration was obtained using the stock concentrations determined with the BCA assay. Therefore this concentration was actually higher than the same concentration in experiment 1. In addition to the first release experiment, Dex/Gel-TA and Dex/Hep-TA hydrogels were included as a condition and also anti-TrkA was included as a neutrally charged VHH.

The measurements on day 7 were performed with PBS that has been surrounding the gel for 72 hours instead of 24 hours, which is something to take into account.

For the hydrogels (mainly) based on Dex-TA, the release profiles in figure 3.3 were obtained. The release profiles of all three of the Dex-TA based hydrogels show a high release on day 1, after which the daily release stabilises and remains almost the same for the other days.

When the Dex/Gel-TA hydrogel in figure 3.3a is compared to the regular Dex-TA hydrogel in figure 3.3c, it can be seen that the addition of gelatin leads to a lower release of anti-TNFα VHHs. The release of anti-MMP9 VHHs from Dex/Gel-TA hydrogel is a bit lower than from Dex-TA hydrogel. However, the release of almost neutral anti-TrkA VHHs is also lower from the Dex/Gel-TA hydrogel compared to Dex-TA hydrogel. Therefore it seems as if the positive charge of gelatin still led to an increase in anti-MMP9 VHH release. This is according to the expectations based on the zeta potentials of the polymers. In figure 3.3b, the addition of heparin to the Dex/Hep-TA hydrogel clearly leads to a lower release of anti-MMP9 VHHs compared to the Dex-TA hydrogel in figure 3.3c. The release of anti-TNFα does not seem to be affected by the addition of heparin at first sight. However, when the release of anti-TNFα is related to the release of neutral anti-TrkA VHHs, a slight increase in anti-TNFα VHH release can be observed. The effect of the addition of heparin on the release profiles was also according to the expectations based on the zeta potentials of the polymers.

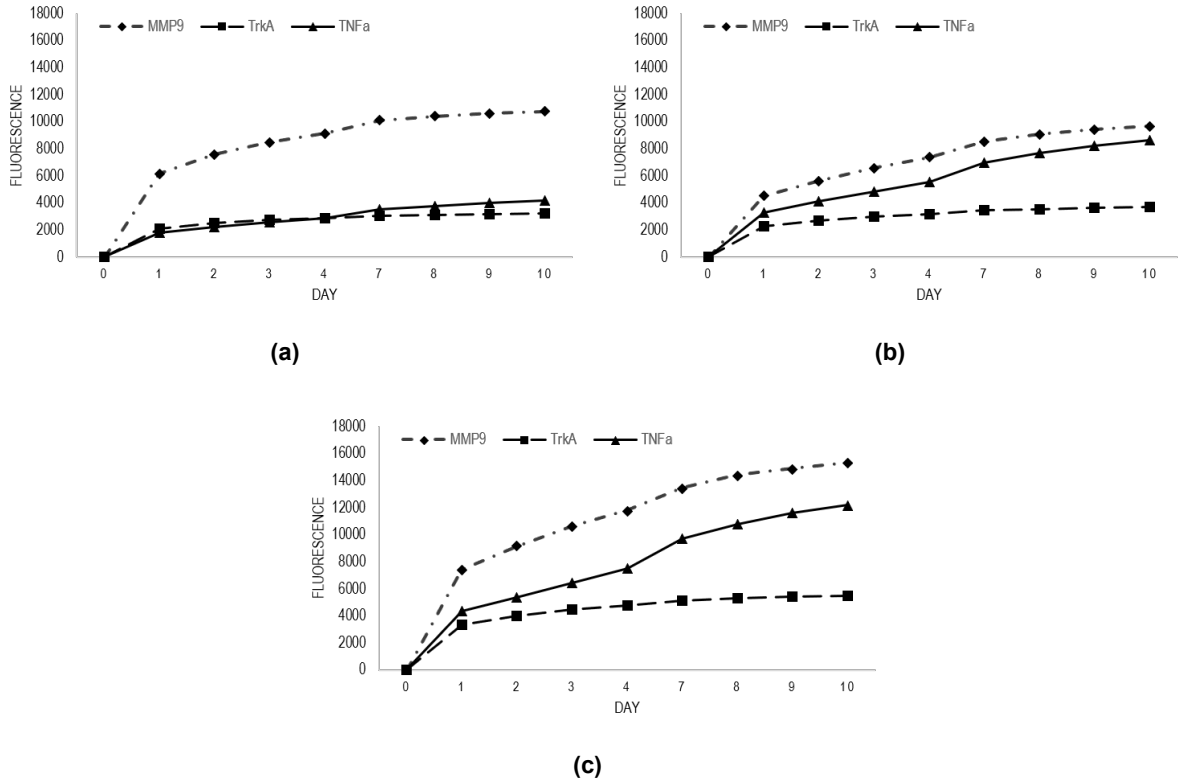

Figure 3.3: The cumulative release profile of anti-MMP9, anti-TrkA and anti-TNFα VHHs from **(a)** Dex/Gel-TA, **(b)** Dex/Hep-TA and **(c)** Dex-TA hydrogels over a time frame of 10 days.

When looking at the release profiles of HA-TA and CS-TA hydrogels in figure 3.4, it is immediately clear that they are almost identical. Since the zeta potentials of both polymers are quite negative, this is according to expectations. However, compared to the Dex-TA type of hydrogels the pattern is quite different. The HA-TA and CS-TA hydrogels show a slow release for the first two days, after which the release slightly increases, and then slowly decreases again.

When comparing the release of the different types of VHHs in these hydrogels to their release in the Dex-TA based hydrogels, it stands out that each of the VHH types is released significantly less in the HA-TA and CS-TA hydrogels. Furthermore, figure 3.4 shows that there is no clear difference between HA-TA and CS-TA when comparing the release of anti-MMP9 and anti-TNFα VHHs. The overall release of the VHHs is slightly higher with the CS-TA hydrogel compared to the HA-TA hydrogel. Based on the zeta potentials of the polymers, CS-TA is expected to release more anti-TNFα VHHs and less anti-MMP9 VHHs compared to HA-TA. However, it could also be possible that from a certain zeta potential the effect of electrostatic interactions no longer increases.

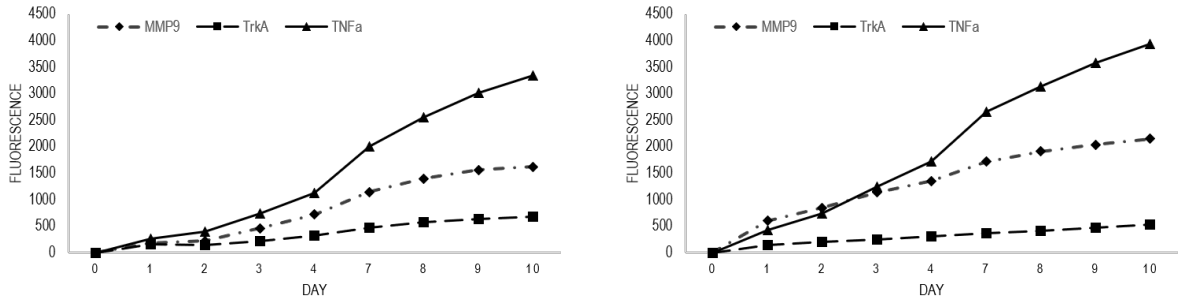

(a) **(b)**

Figure 3.4: The cumulative release profile of anti-MMP9, anti-TrkA and anti-TNFα VHHs from **(a)** HA-TA and **(b)** CS-TA hydrogels over a time frame of 10 days.

The results of the fluorescence intensity measurements of the hydrogels themselves are presented as a percentage of the fluorescence intensity at day 0. In figure 3.5, which shows the Dex-TA based hydrogels, it can be seen that there are fluctuations, similar to the first release experiment. Despite the fluctuations, this data can still be used to gain insight in the amount of VHHs that were released after 10 days. For all types of VHHs, at least 45 percent of the VHHs was still present in each of the Dex-TA based hydrogels at this point. The release profiles obtained from the fluorescence intensity measurements of the hydrogels themselves show contradictory results compared to the PBS sample measurements. In figure 3.5 it can be seen that from the Dex/Gel-TA hydrogel less anti-MMP9 VHHs were released than from the Dex/Hep-TA hydrogel. This is even clearer in the graphs in appendix A.6 that show the absolute fluorescence intensity. However, the fluctuations can be an explanation for these contradictory findings and due to these fluctuations the measurements cannot be seen as reliable.

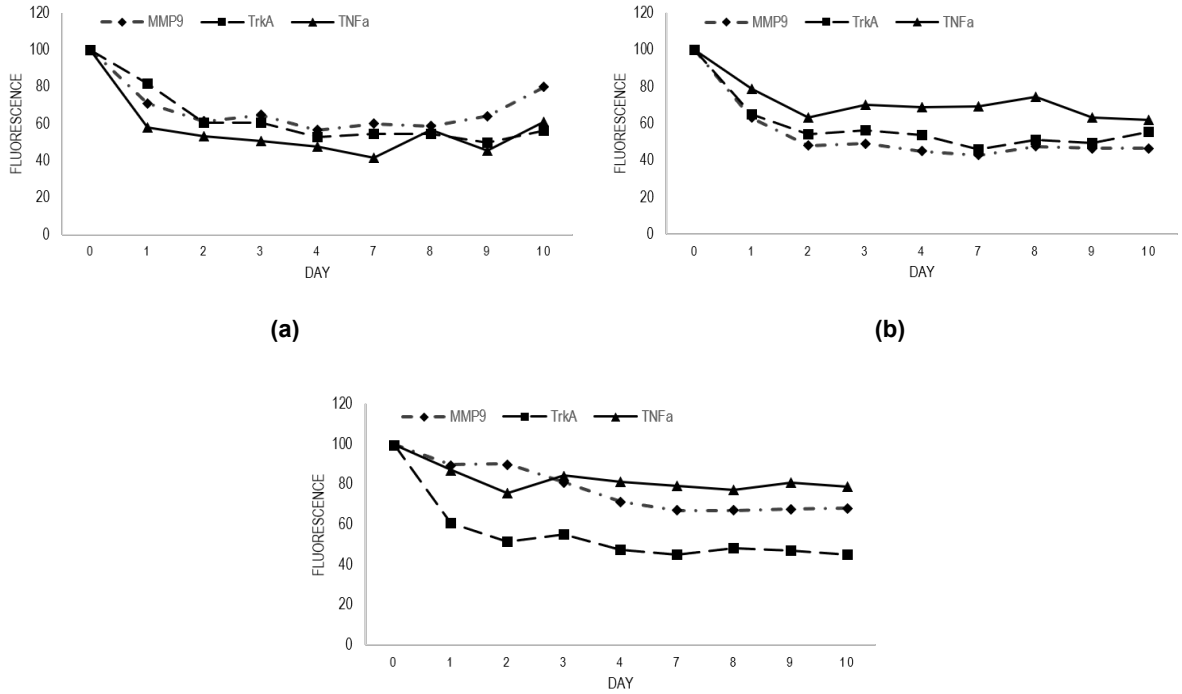

Figure 3.5: The fluorescence intensity of the **(a)** Dex/Gel-TA, **(b)** Dex/Hep-TA and **(c)** Dex-TA hydrogels themselves presented as a percentage of the fluorescence intensity at day 0.

The graphs in figure 3.6 show the fluorescence intensity of the HA-TA and CS-TA hydrogels themselves. These measurements show even more fluctuations compared to the Dex-TA based hydrogels, which leads to fluorescence intensities higher than the initial value at day 0. Therefore it is not possible to make a statement about the percentage of VHHs that is still present in the hydrogels after 10 days.

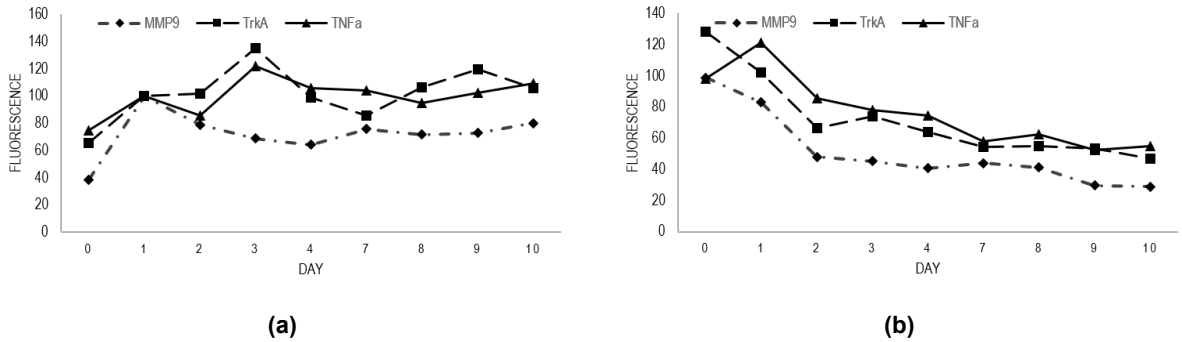

Figure 3.6: The fluorescence intensity of the **(a)** HA-TA and **(b)** CS-TA hydrogels themselves presented as a percentage of the fluorescence intensity at day 0.

3.3 VHH presence in release samples

Next to the fluorescence intensity of the PBS samples, the presence of VHHs in the collected PBS samples of the second release experiment was also determined with an ELISA assay. The results from this assay show that there were indeed VHHs present in the collected samples. The

amount of absorbance that was measured in the samples from Dex-TA type of hydrogels corresponds to the findings of the second release experiment. In figures 3.7, 3.8 and 3.9 the graphs with the absorbance measurements and the graphs with the fluorescence intensity measurements can be seen side by side. Compared to the standard Dex-TA hydrogel, addition of gelatin seems to increase the release of anti-MMP9 VHHs and decrease the release of anti-TrkA and anti-TNFα VHHs. The addition of heparin to the Dex-TA hydrogel seems to do the exact opposite. This corresponds to the findings from the second release experiment and is also expected based on the zeta potentials of the polymers.

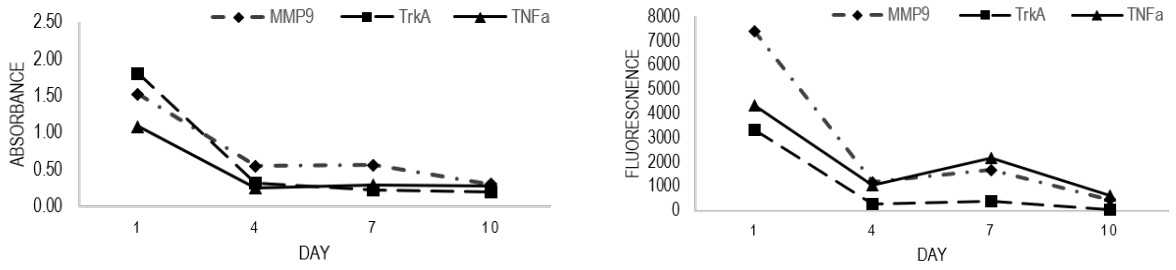

(a) **(b)**

Figure 3.7: A comparison between the absorbance measurements of the samples from day 1, 4, 7 and 10 and the corresponding fluorescence measurements of the Dex-TA hydrogel.

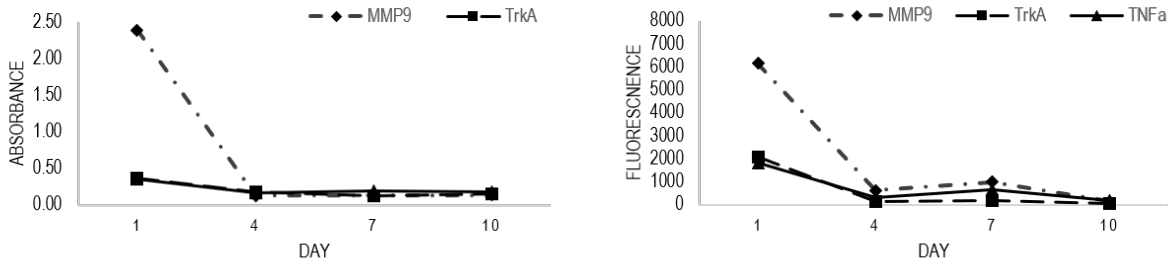

(a) **(b)**

Figure 3.8: A comparison between the absorbance measurements of the samples from day 1, 4, 7 and 10 and the corresponding fluorescence measurements of the Dex/Gel-TA hydrogel.

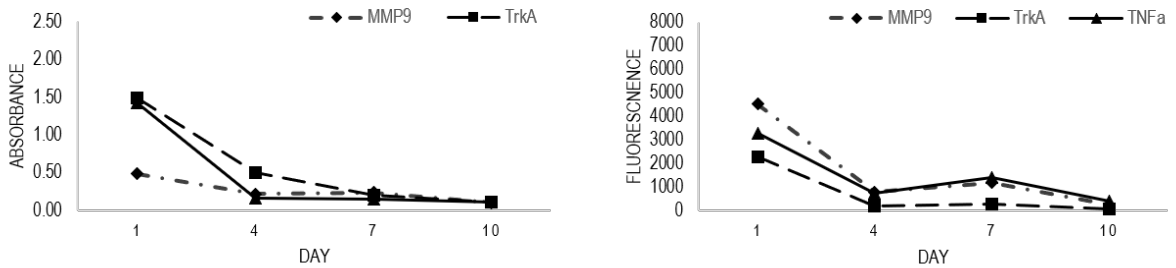

(a) **(b)**

Figure 3.9: A comparison between the absorbance measurements of the samples from day 1, 4, 7 and 10 and the corresponding fluorescence measurements of the Dex/Hep-TA hydrogel.

With respect to the graphs of the HA-TA and CS-TA hydrogel in figures 3.10 and 3.11, the measured absorbance is not in accordance with the earlier discussed fluorescence measurements. Anti-TrkA VHHs showed an almost constant release in these fluorescence measurements, while the absorbance measurements clearly show an increase in release until day 7 and day 4 for HA-TA and CS-TA respectively. For the anti-TNFα and anti-MMP9 VHHs the absorbance measurements are also not in accordance with the fluorescence intensity measurements. The release of anti-TNFα VHHs decreases in the HA-TA hydrogel and remains the same in the CS-TA hydrogel on day 7 according to the absorbance measurements. However, the fluorescence measurements did show an increased release on day 7, which was also expected, since this PBS was not renewed for 72 hours. Almost the same phenomenon was visible with the anti-MMP9 VHHs.

Calibration curves for each of the VHH types are shown in appendix A.7, to provide insight in the amount of VHHs present in the collected samples. The measurements for these calibration curves were also considered as positive controls. The highest concentration of the positive controls was calculated to be higher than the highest possible VHH concentration in the PBS samples. However, the measured absorbance values of these positive controls were extremely low, especially compared to the samples that were released from the hydrogels. Since the absorbance and fluorescence intensity measurements show a high similarity, the absorbance measurements still seem reliable, despite the low absorbance values of the positive controls.

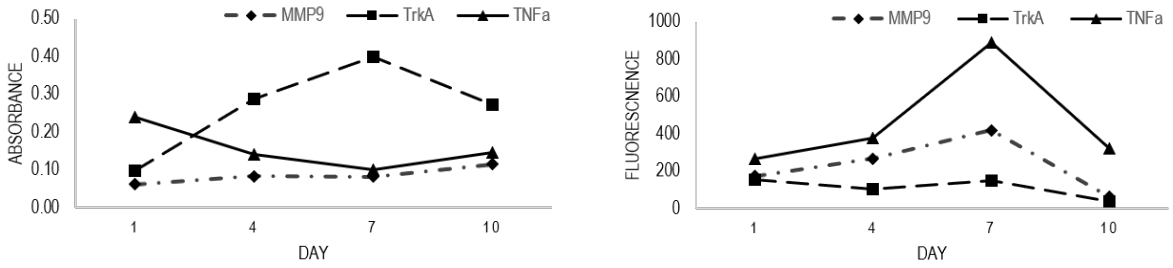

(a) **(b)**

Figure 3.10: A comparison between the absorbance measurements of the samples from day 1, 4, 7 and 10 and the corresponding fluorescence measurements of the HA-TA hydrogel.

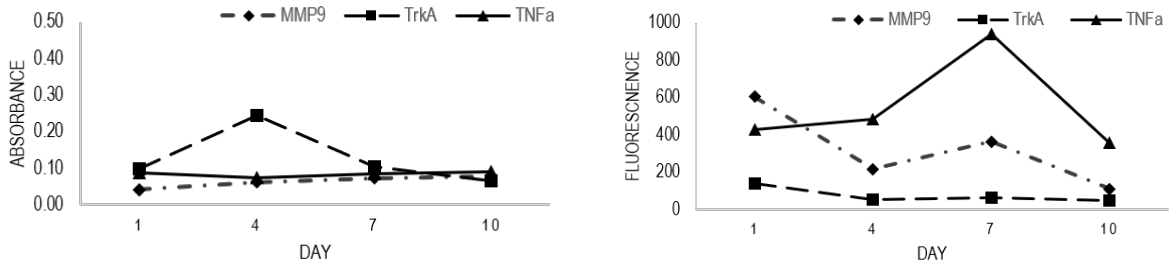

(a) **(b)**

Figure 3.11: A comparison between the absorbance measurements of the samples from day 1, 4, 7 and 10 and the corresponding fluorescence measurements of the CS-TA hydrogel.

3.4 Binding specificity of the VHHs

In addition to the absorbance measurements that determined the VHH presence in the collected PBS samples, a second ELISA assay was performed to determine if the released VHHs were still able to bind to their corresponding target. In figure 3.12 the results of this assay are shown for the Dex-TA based hydrogels. These graphs show very low absorbance of the samples obtained from the second release experiment. The measured absorbance of the VHHs released from Dex/Gel-TA and Dex/Hep-TA is almost zero, while the VHHs released from the standard Dex-TA hydrogel give absorbance values between 0.01 and 0.25. The control samples measured in this experiment, however, also show very low absorbance for each of the VHHs. These control samples consist of 16 µg/mL labelled and unlabelled VHH samples. Only the unlabelled anti-TNFα VHHs show a relatively high absorbance value compared to the other types of VHHs. The extremely low absorbance values would indicate that the VHHs were not able to bind to their target after release from the hydrogels, which was against expectations. When comparing the two control groups, it stands out that the unlabelled VHHs have a higher absorbance for each of the VHH types, which was expected due to a possible influence of the FITC dye on the binding affinity.

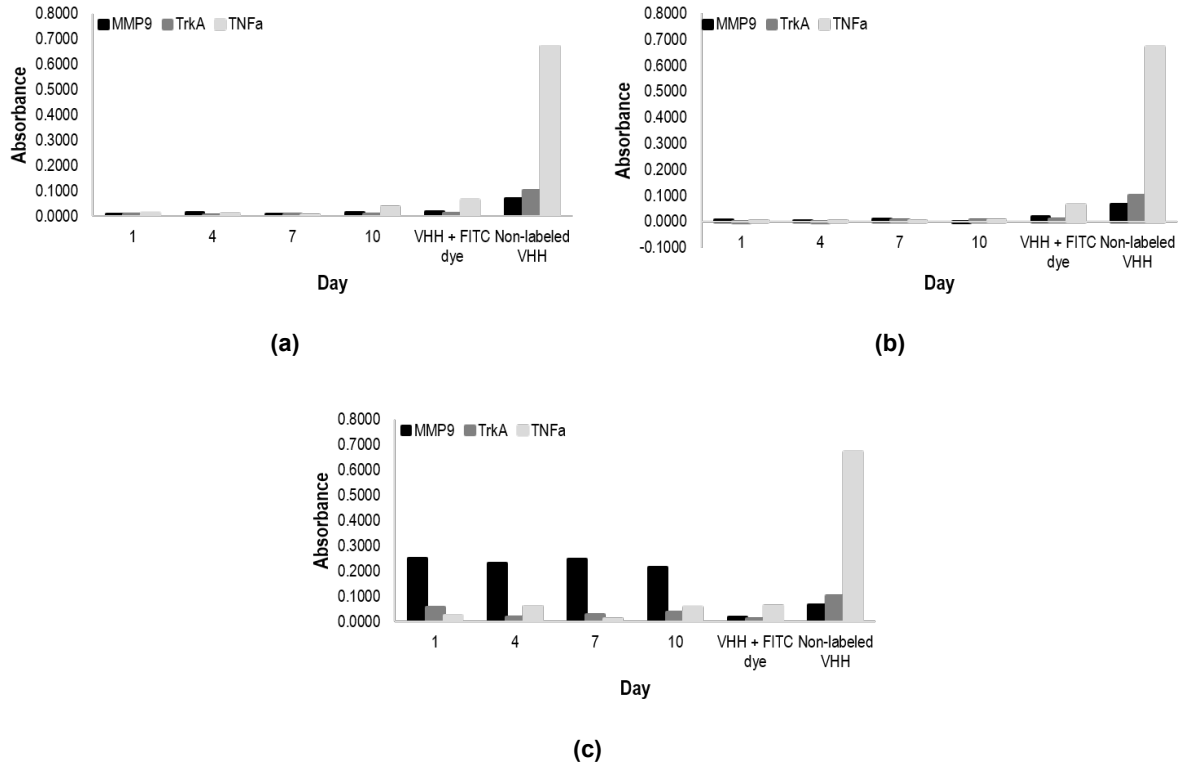

Figure 3.12: The measured absorbance for **(a)** Dex/Gel-TA, **(b)** Dex/Hep-TA and **(c)** Dex-TA, to determine if the VHHs were still able to bind to their target after release from these hydrogels.

The VHHs released from HA-TA and CS-TA show identical results with the Dex/Gel-TA and Dex-Hep-TA hydrogels. With these hydrogels the absorbance of the released VHHs is also almost zero, as shown in figure 3.13. These results were also not as expected.

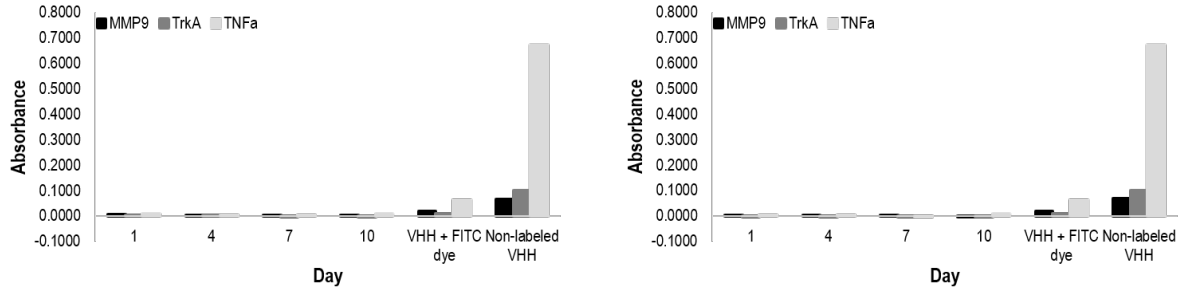

(a) (b)

Figure 3.13: The measured absorbance for **(a)** HA-TA and **(b)** CS-TA, to determine if the VHHs were still able to bind to their target after release from these hydrogels.

3.5 VHH interaction with human cartilage

For studying the interaction of two different VHHs with human cartilage, two experiments were performed. In the first experiment cartilage samples were placed in a wells plate, to which the VHHs were added. With fluorescence microscopy the fluorescence intensity of the cartilage samples was monitored over time. In the second experiment cartilage samples were also placed in a wells plate, to which VHHs were added. This time, however, the samples were fixated at different time points and processed into 5 µm cryosections that were analyzed with fluorescence microscopy (EVOS).

3.5.1 Experiment 1

The results of the first experiment show that all of the VHHs indeed show some form of interaction with the cartilage samples. The point where the most of each different type of VHH interacts with the cartilage sample is between two and four hours, since the fluorescence intensity is at its highest at these time points. This is shown in figures 3.14, 3.15 and 3.16. After this point the fluorescence intensity decreases again in all of the samples. From this experiment it could not be determined if the VHHs were actively bound to the tissue or that they passively moved in to the tissue.

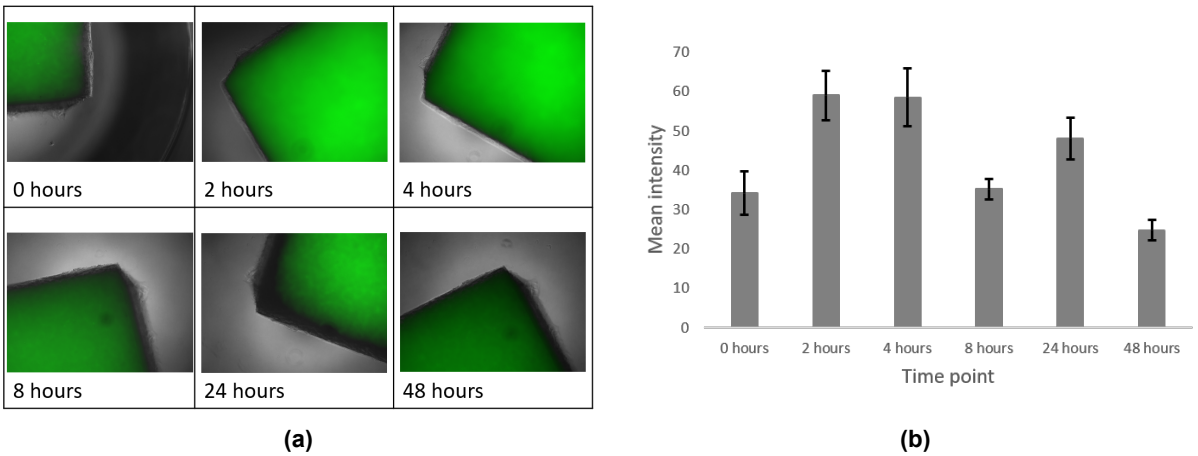

(a) (b)

Figure 3.14: **(a)** An overview of the fluorescence intensity of the cartilage samples with anti-MMP9 VHHs added to them over time **(b)** Quantified intensities of the cartilage samples presented in a bar graph.

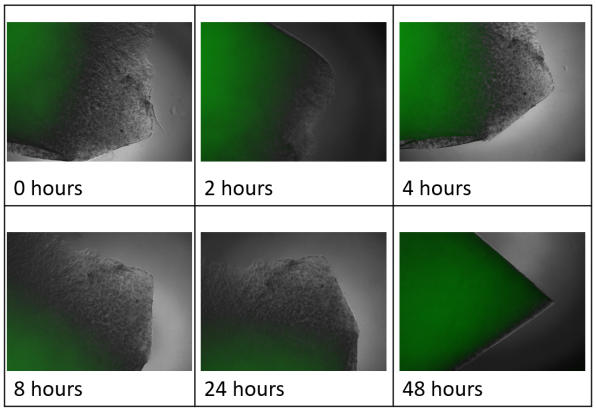

(a)

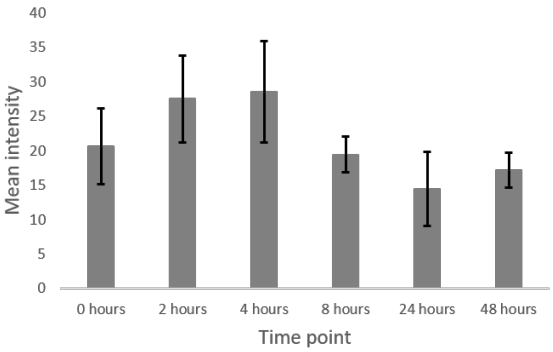

(b)

Figure 3.15: (a) An overview of the fluorescence intensity of the cartilage samples with anti-TrkA VHHs added to them over time **(b)** Quantified intensities of the cartilage samples presented in a bar graph.

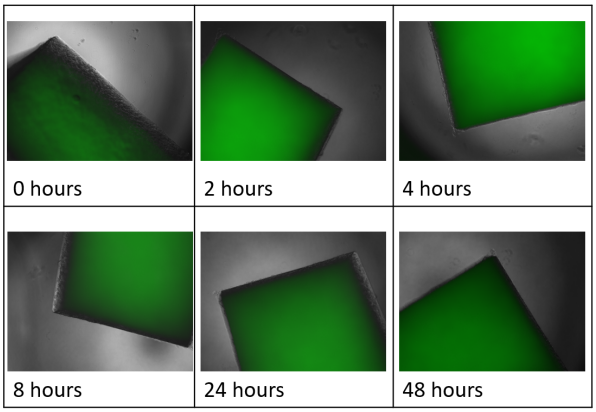

(a)

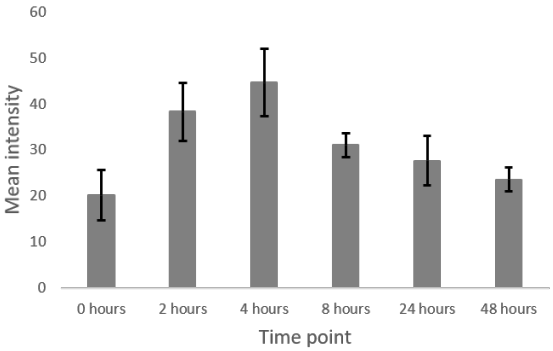

(b)

Figure 3.16: (a) An overview of the fluorescence intensity of the cartilage samples with anti-TNFα VHH added to them over time **(b)** Quantified intensities of the cartilage samples presented in a bar graph.

3.5.2 Experiment 2

To further study the interactions between VHHs and human cartilage that were shown in the first experiment, the experiment was repeated. This time cryosections of the cartilage tissue were made and imaged with a fluorescence microscope (EVOS). The results of this experiment did not show any difference in fluorescence intensity between the cartilage samples with VHH added to them and the negative control. This is visible in figure 3.17, in which the cartilage sample with anti-MMP9 VHHs that was fixated after 4 hours can be seen next to the negative control, with two different magnifications being used.

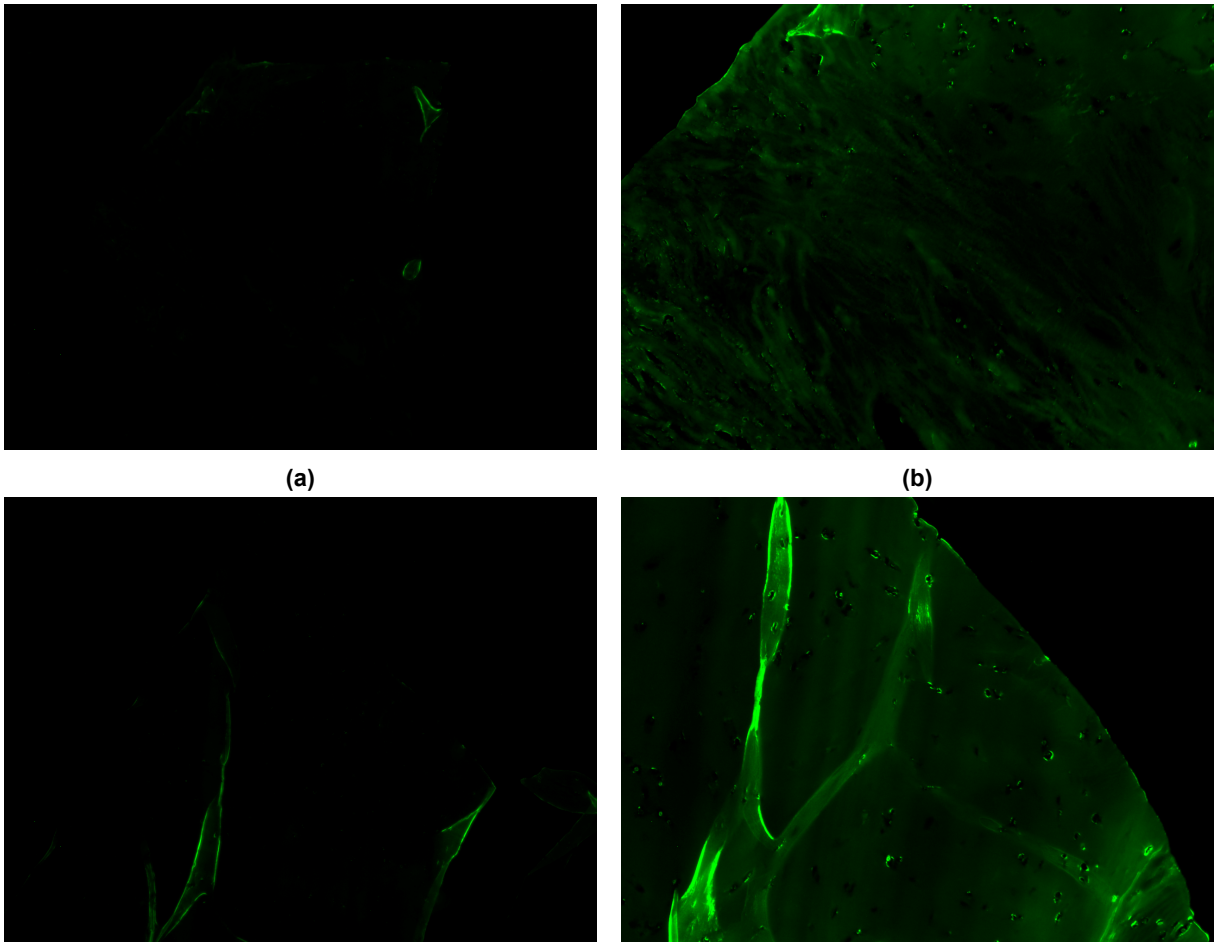

Figure 3.17: **(a)** GFP channel images of cartilage tissue incubated with anti-MMP9 VHHs fixated after 4 hours at 4x magnification and **(b)** 10x magnification. **(c)** GFP channel images of the control cartilage tissue fixated after 4 hours at 4x magnification and **(d)** 10x magnification.

The intensity of the fluorescent signal was also quantified with ImageJ for each of the images, which is shown in figure 3.18. The diagrams for both used magnifications do not show any clear difference between the samples with VHH added and the negative control, which is in accordance with what can be seen in figure 3.17. The second experiment therefore does not provide additional insights into the interactions between VHHs and human cartilage.

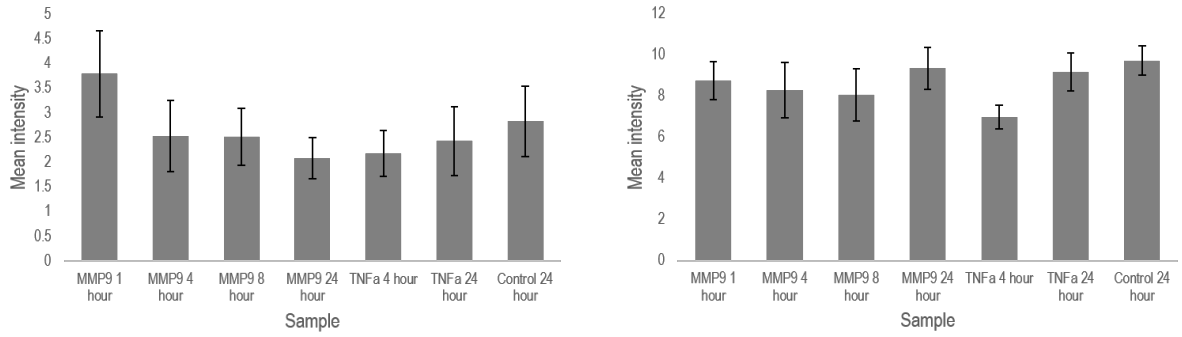

(a) **(b)**

Figure 3.18: (a) The mean intensities of the GFP channel images from all cartilage samples imaged with a 4x objective. **(b)** The mean intensities of the GFP channel images from all cartilage samples imaged with a 10x objective.

4 DISCUSSION

4.1 VHH release profile measurements

The fluorescence intensity of the PBS supernatants and the fluorescence intensity of the hydrogels themselves were both measured with the VICTOR3 Multilabel Plate Reader, as described in section 2.4. The fluorescence intensity measurements of the hydrogels themselves, however, did show many fluctuations. The experiment was performed in duplicate, so it was not possible to identify which of the two measurements was the outlier in most of the cases. Since it is theoretically not possible for the fluorescent signal to increase over time or to become a negative value, these measurements were considered as inaccurate. Therefore conclusions about the release of the VHHs from the hydrogels can only be based on the daily measurements of the PBS in the wells for both experiment 1 and experiment 2. A possible explanation for these fluctuations can be that the hydrogels did not completely fill the wells and were therefore able to move. This could result in different measurement points during the experiment, which could explain the fluctuations if the VHHs were not completely homogeneously distributed throughout the hydrogels.
In addition, the hydrogels are spherically shaped. Therefore the thickness of the hydrogels is decreasing towards the edges of the hydrogels, which probably means that there are less VHHs at the edges compared to the center of the hydrogel. This could have an influence on the measurements, which could explain the fluctuations in the measurements over time.
Furthermore, the measured fluorescence intensity of the negative control (hydrogel without VHHs) was subtracted from the actual measurements, to correct for the background signal. The values of these negative control measurements ranged from 984 to 10557 in the first release experiment. In some cases these values were higher than the actual measurements of the hydrogels with VHHs incorporated, which resulted in negative fluorescence intensities. This phenomenon also provides insight into the range of fluctuations in the fluorescence intensity measurements, since the measured values of the negative control should remain constant.

Something else to take into account is that the polymer and VHH charges could only be based on values found in literature, since it was not possible to measure zeta potentials due to circumstances. Based on pKa values of the side chains of the polymers, it is expected that Heparin-Tyramine is more negative than Hyaluronic Acid-Tyramine. This is opposite to the Zeta potentials found in literature that are shown in table 1.1. The zeta potentials of some polymers also vary quite a bit between some publications. For Dex-TA two zeta potential values were found, between which there was a -18 mV difference [27, 37]. For HA-TA a difference in zeta potential of -33 mV was found between two publications. This shows the importance of measuring the zeta potentials of the exact polymers used in this research. The effect on the charge of gelatin and heparin addition to Dex-TA hydrogels could also not be determined in this research. Therefore measuring the zeta potentials of the used polymer solutions and VHHs could be extremely useful in future research.

Something that could have an influence on the VHH release from hydrogels is the fact that tyramine-functionalized polymers can covalently bind with tyrosine in the extracellular matrix of

cartilage [38]. This suggests that tyrosine groups present in VHHs are able to bind covalently to the tyramine groups attached to the polymer backbone. This interaction is visualized in figure 4.1. Depending on the amount of tyrosine groups present in a particular VHH, the possible binding of VHH to the polymer chain can negatively influence the release of the VHHs. This phenomenon could explain the fact that the fluorescence measurements in figure 3.5 show that there were still quite some VHHs present in the hydrogels after 10 days.

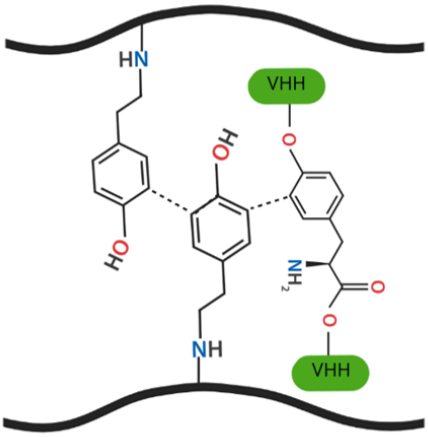

Figure 4.1: A schematic overview of the possible interactions between tyramine groups bound to the polymer backbone and tyrosine groups present in the VHHs.

Another factor that can influence the VHH release from hydrogels is the mesh size. As explained in section 1.3, a mesh size bigger than the VHH size leads to diffusion based release. A smaller mesh size leads to slower release and when the mesh size is smaller than the VHH size, the VHHs will not be able to move freely through the hydrogel anymore [26]. The effect of the mesh size on diffusion is visualized in figure 4.2. In this research the mesh sizes of the used hydrogels are unknown and therefore it is not possible to make accurate statements about the effect of the mesh sizes. However, a difference in mesh size could be a possible explanation for the fact that the Dex-TA based hydrogels show more overall release compared to the HA-TA and CS-TA hydrogels.

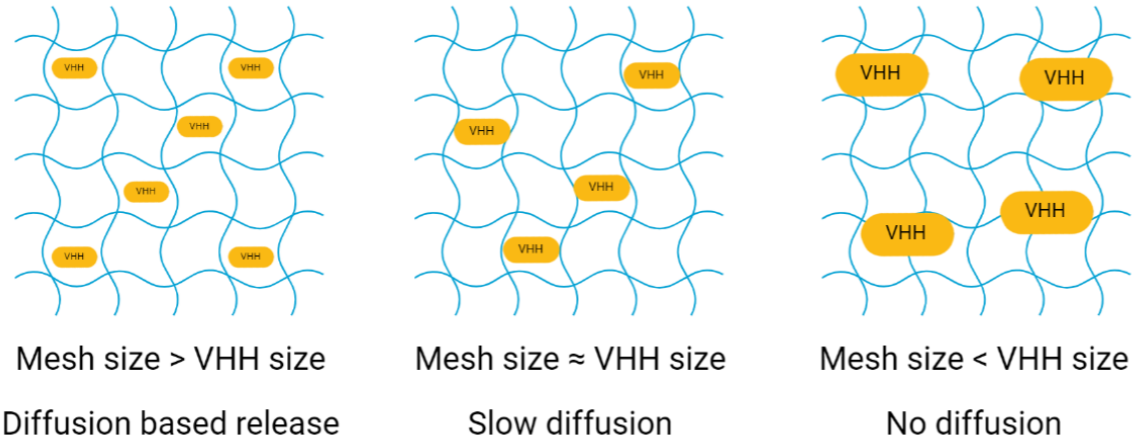

Figure 4.2: A schematic representation of the effect of the mesh size of the hydrogel on the diffusion of VHHs through the hydrogel.

4.2 VHH presence and binding specificity

The VHHs used in this research were fluorescently labelled with FITC. FITC-NHS conjugates to free amino groups of lysine. If these lysine groups are only easily available near or in the antigen binding site of the VHH, this could have a negative influence on the binding affinity of the VHH for its target [39, 40]. This could be an explanation for the lower absorbance measured in the fluorescently labelled control group compared to the unlabelled control group in the ELISA assay performed to determine VHH binding specificity after release. However, complete loss of binding affinity has not yet been reported in current literature.

In the ELISA assay performed to determine the binding specificity of the VHHs after release, not only the absorbance of the actual samples, but also the absorbance of the control groups was significantly lower than expected. In this ELISA assay the plate was coated with the targets, after which the PBS samples that contained VHHs according to section 3.3 were added. To detect the bound VHHs, goat anti-llama IgG was added. If the VHH concentration that still had binding affinity to their target was already lower due to FITC conjugation and on top of that the binding of goat anti-llama IgG to the VHHs was also lower than expected, it could be that the VHH concentration was lower than the detection limit of the Multiskan GO. As stated earlier, complete loss of binding affinity after fluorescent labelling has not yet been reported and therefore a technological issue in the execution of the assay also seems plausible.

As stated in section 3.3, the labelled positive control samples of the ELISA assay to determine the presence of VHHs in the collected PBS samples showed low absorbance values. Since the VHHs in the actual samples of this experiment were also labelled with FITC, this could not be explained by loss of binding affinity due to FITC conjugation. A technological issue with the ELISA assay therefore seems likely. However, the similarities between the absorbance and fluorescence intensity measurements seem to indicate that the ELISA assay results are reliable.

4.3 VHH interaction with human cartilage

In the experiments with human cartilage autofluorescence was visible in the negative control cartilage tissues. The main contributor to cartilage autofluorescence is collagen[41]. The autofluorescence in the first experiment was quite a bit lower than the fluorescence intensity of the samples. Therefore the results could still be analyzed after subtraction of the fluorescence intensity of the negative control. In the second experiment, however, the autofluorescence intensity was approximately equal to the fluorescence intensity of the samples. In this experiment the autofluorescence could have been increased by the fixation process. Fixation with paraformaldehyde was reported to increase autofluorescence [42].

In the first experiment a VHH concentration of 10 µg/mL was used. This resulted in an extremely high fluorescence intensity of the cartilage tissues. This made it difficult to evaluate the VHH interactions between different parts of the tissue, so no clear statements about this could be made in this research. Due to this high fluorescence intensity, the VHH concentration in the second experiment was altered to 1 µg/mL. However, in the second experiment no fluorescence was observed apart from the autofluorescence of the cartilage tissue. It could be that the 1 µg/mL VHH concentration was not high enough to detect the fluorescence of the VHHs.

Furthermore, it could be the case that FITC dye is not very suitable for fluorescence imaging. FITC is highly sensitive to photobleaching and during cryosectioning the samples were exposed to light for a short time, although this light did not directly shine on the samples. Mounting medium could be used in future research to prevent photobleaching. In addition, FITC is

extremely sensitive to pH changes and it is is relatively dim [43]. These properties could all explain the fact that there was no fluorescence visible in the cartilage tissues apart from the autofluorescence of the cartilage tissues.

5 CONCLUSION

The release of VHH nanobodies from the hydrogels with a Dex-TA based polymer backbone seems to be affected by electrostatic interactions between the polymer backbone and the incorporated VHHs. The effect of the electrostatic interactions is not as great as hypothesized. However, Dex-TA based hydrogels still show great potential for hydrogel based VHH release systems, since it seems that release can be tuned by varying the polymer charge. For HA-TA and CS-TA hydrogels the electrostatic interactions do not seem to have an effect on the VHH release.

Based on this research, it could be concluded that the VHHs had no binding affinity to their targets after release. However, to confirm or refute these findings, further research is necessary.

Finally, it can be concluded that the VHHs show some form of interaction with human cartilage. The mechanism of this interaction is still unclear, so further research is necessary to gain more insight into this.

6 RECOMMENDATIONS

This research shows the potential of Dex/Gel-TA and Dex/Hep-TA hydrogels for VHH release based on charge. However, only a 95:5 polymer ratio was used for both of these hydrogels. To further study the potential of these two types of hydrogel as VHH release systems, it is important to study the VHH release profiles and the zeta potentials for a range of different polymer ratios. This way, the effect of the addition of gelatin and heparin on the zeta potential and with it the polymer charge, can be measured. It seems plausible that by varying the polymer charge, optimized release systems for a wide range of VHHs can be developed. This can be of potential use in the treatment of OA.

Another point that could be looked into in future research is controlling the VHH release during the first 24 hours. During the first 24 hours the VHHs are released in an initial burst. When a constant administration of VHHs is desired, this initial burst needs to be reduced. This can be done by increasing the initial monomer concentration in the hydrogel [44]. In future research this is something to take into consideration.

For assessing the binding specificity of the VHHs after release from the hydrogels, it could be beneficial to also perform this experiment with non-labelled VHHs. This way, the effect of the fluorescent label on the binding affinity could be determined. In addition, an experiment set up in this form will provide insight into the actual binding affinity in vivo, since it is likely that only non-labelled VHHs will be administered into the human body for therapeutic purposes.

7 ACKNOWLEDGEMENTS

First of all I would like to thank Prof. Dr. Marcel Karperien for giving me the opportunity to perform my bachelor assignment in the Developmental BioEngineering group. His feedback during the assignment was also really appreciated.

In addition, I would like to express my gratitude to my daily supervisors Dr. Bram Zoetebier and Lisanne Morshuis for their excellent guidance and feedback during the assignment. I would also like to thank them for providing the necessary materials for my research, including the polymers and the VHHs.

Furthermore, I would like to thank Dr. Ruchi Bansal for being part of the examination committee and for her helpful feedback during the assignment.

Finally, I would like to thank the complete Developmental BioEngineering group for providing a pleasant working environment and for making the labs available for my research.

REFERENCES

1. Martínez-Moreno D, Jiménez G, Gálvez-Martín P, Rus G, and Marchal JA. Cartilage biomechanics: A key factor for osteoarthritis regenerative medicine. 2019 Jun. DOI: 10.1016/j.bbadis.2019.03.011
2. De Giacomo AF, Banffy MB, and ElAttrache NS. Biologics in orthopaedic surgery. *Biologics in Orthopaedic Surgery*. Elsevier, 2018 Jan :27–47. DOI: 10.1016/B978-0-323-55140-3.00004-7
3. Chen D, Shen J, Zhao W, Wang T, Han L, Hamilton JL, and Im HJ. Osteoarthritis: Toward a comprehensive understanding of pathological mechanism. 2017 Jan. DOI: 10.1038/boneres.2016.44. Available from: www.nature.com/boneres
4. Artrose | Cijfers & Context | Huidige situatie | Volksgezondheidenzorg.info. Available from: https://www.volksgezondheidenzorg.info/onderwerp/artrose/cijfers-context/huidige-situatie%7B%5C#%7Dnode-prevalentie-en-aantal-nieuwe-gevallen-van-artrose-huisartsenpraktijk [Accessed on: 2021 Apr 21]
5. Xia B, Di Chen, Zhang J, Hu S, Jin H, and Tong P. Osteoarthritis Pathogenesis: A Review of Molecular Mechanisms. 2014 Nov. DOI: 10.1007/s00223-014-9917-9. Available from: https://link-springer-com.ezproxy2.utwente.nl/article/10.1007/s00223-014-9917-9
6. Glyn-Jones S, Palmer AJ, Agricola R, Price AJ, Vincent TL, Weinans H, and Carr AJ. Osteoarthritis. *The Lancet*. Vol. 386. 9991. Lancet Publishing Group, 2015 Jul :376–87. DOI: 10.1016/S0140-6736(14)60802-3
7. Zheng S, Hunter DJ, Xu J, and Ding C. Monoclonal antibodies for the treatment of osteoarthritis. 2016 Dec. DOI: 10.1080/14712598.2016.1229774. Available from: https://www.tandfonline.com/action/journalInformation?journalCode=iebt20
8. Jovčevska I and Muyldermans S. The Therapeutic Potential of Nanobodies. 2020 Feb. DOI: 10.1007/s40259-019-00392-z. Available from: https://pubmed-ncbi-nlm-nih-gov.ezproxy2.utwente.nl/31686399/
9. Rodrigues E. Single domain antibodies in tissue engineering. English. PhD thesis. University of Twente, 2014 Sep. DOI: 10.3990/1.9789036537353
10. Van Audenhove I and Gettemans J. Nanobodies as Versatile Tools to Understand, Diagnose, Visualize and Treat Cancer. 2016 Jun. DOI: 10.1016/j.ebiom.2016.04.028
11. Muyldermans S, Cambillau C, and Wyns L. Recognition of antigens by single-domain antibody fragments: The superfluous luxury of paired domains. 2001 Apr. DOI: 10.1016/S0968-0004(01)01790-X
12. Wojdasiewicz P, Poniatowski ŁA, and Szukiewicz D. The role of inflammatory and anti-inflammatory cytokines in the pathogenesis of osteoarthritis. 2014. DOI: 10.1155/2014/561459. Available from: /pmc/articles/PMC4021678/%20/pmc/articles/PMC4021678/?report=abstract%20https://www.ncbi.nlm.nih.gov/pmc/articles/PMC4021678/

13. Zeng GQ, Chen AB, Li W, Song JH, and Gao CY. High MMP-1, MMP-2, and MMP-9 protein levels in osteoarthritis. Genetics and Molecular Research 2015 Nov; 14:14811–22. DOI: 10.4238/2015.November.18.46. Available from: https://pubmed.ncbi.nlm.nih.gov/26600542/

14. Li H, Miao SB, Dong LH, Shu Y nan, Shao DC, Chen BC, Han M, and Zhang Y. Clinicopathological correlation of Krüppel-like factor 5 and matrix metalloproteinase-9 expression and cartilage degeneration in human osteoarthritis. Pathology Research and Practice 2012 Jan; 208:9–14. DOI: 10.1016/j.prp.2011.09.015

15. Kim KS, Lee YA, Choi HM, Yoo MC, and Yang HI. Implication of MMP-9 and urokinase plasminogen activator (uPA) in the activation of pro-matrix metalloproteinase (MMP)-13. Rheumatology International 2012 Oct; 32:3069–75. DOI: 10.1007/s00296-011-2095-4. Available from: https://link.springer.com/article/10.1007/s00296-011-2095-4

16. Rukwied R, Mayer A, Kluschina O, Obreja O, Schley M, and Schmelz M. NGF induces non-inflammatory localized and lasting mechanical and thermal hypersensitivity in human skin. Pain 2010 Mar; 148:407–13. DOI: 10.1016/j.pain.2009.11.022

17. Jiang Y and Tuan RS. Role of NGF-TrkA signaling in calcification of articular chondrocytes. FASEB Journal 2019 Sep; 33:10231–9. DOI: 10.1096/fj.201900970. Available from: www.fasebj.org

18. Shang X, Wang Z, and Tao H. Mechanism and therapeutic effectiveness of nerve growth factor in osteoarthritis pain. Therapeutics and Clinical Risk Management 2017 Aug; 13:951–6. DOI: 10.2147/TCRM.S139814. Available from: /pmc/articles/PMC5546917/%20/pmc/articles/PMC5546917/?report=abstract%20https://www.ncbi.nlm.nih.gov/pmc/articles/PMC5546917/

19. Schnitzer TJ and Marks JA. A systematic review of the efficacy and general safety of antibodies to NGF in the treatment of OA of the hip or knee. 2015 Jan. DOI: 10.1016/j.joca.2014.10.003

20. Obeidat AM, Donner A, and Miller RE. An Update on Targets for Treating Osteoarthritis Pain: NGF and TRPV1. Current Treatment Options in Rheumatology 2020 Sep; 6:129–45. DOI: 10.1007/s40674-020-00146-x. Available from: https://www.

21. Xie C and Chen Q. Adipokines: New Therapeutic Target for Osteoarthritis? 2019 Dec. DOI: 10.1007/s11926-019-0868-z. Available from: https://doi.org/10.1007/s11926-019-0868-z

22. Chisari E, Yaghmour KM, and Khan WS. The effects of TNF-alpha inhibition on cartilage: a systematic review of preclinical studies. 2020 May. DOI: 10.1016/j.joca.2019.09.008. Available from: https://doi.org/10.1016/j.joca.2019.09.008

23. Amin S, Rajabnezhad S, and Kohli K. Hydrogels as potential drug delivery systems. Scientific Research and Essay 2009; 3:1175–83. Available from: http://www.academicjournals.org/SRE

24. Ashley GW, Henise J, Reid R, and Santi DV. Hydrogel drug delivery system with predictable and tunable drug release and degradation rates. Proceedings of the National Academy of Sciences of the United States of America 2013 Feb; 110:2318–23. DOI: 10.1073/pnas.1215498110. Available from: www.pnas.org/cgi/doi/10.1073/pnas.1215498110

25. Wang R, Leber N, Buhl C, Verdonschot N, Dijkstra PJ, and Karperien M. Cartilage adhesive and mechanical properties of enzymatically crosslinked polysaccharide tyramine conjugate hydrogels. Polymers for Advanced Technologies 2014; 25:568–74. DOI: 10.1002/pat.3286

26. Li J and Mooney DJ. Designing hydrogels for controlled drug delivery. 2016 Oct. DOI: 10.1038/natrevmats.2016.71. Available from: /pmc/articles/PMC5898614/%20/pmc/articles/PMC5898614/?report=abstract%20https://www.ncbi.nlm.nih.gov/pmc/articles/PMC5898614/

27. Khot S, Rawal SU, and Patel MM. Dissolvable-soluble or biodegradable polymers. *Drug Delivery Devices and Therapeutic Systems*. Elsevier, 2021 Jan :367–94. DOI: 10.1016/b978-0-12-819838-4.00024-9

28. Fakhari A. Biomedical Application of Hyaluronic Acid Nanoparticles. Tech. rep. 2012 May. Available from: https://kuscholarworks.ku.edu/handle/1808/9825

29. Chuang CH, Lin RZ, Tien HW, Chu YC, Li YC, Melero-Martin JM, and Chen YC. Enzymatic regulation of functional vascular networks using gelatin hydrogels. Acta Biomaterialia 2015 Jun; 19:85–99. DOI: 10.1016/j.actbio.2015.02.024. Available from: /pmc/articles/PMC4589259/%20/pmc/articles/PMC4589259/?report=abstract%20https://www.ncbi.nlm.nih.gov/pmc/articles/PMC4589259/

30. Lee Y, Le Thi P, Seon GM, Ryu SB, Brophy CM, Kim YT, Park JC, Park KD, Cheung-Flynn J, and Sung HJ. Heparin-functionalized polymer graft surface eluting MK2 inhibitory peptide to improve hemocompatibility and anti-neointimal activity. Journal of Controlled Release 2017 Nov; 266:321–30. DOI: 10.1016/j.jconrel.2017.10.002. Available from: http://europepmc.org/articles/pmc5723561%20http://europepmc.org/abstract/MED/28987880%20/articles/PMC5723561/?report=abstract%20https://europepmc.org/articles/PMC5723561/

31. Khanmohammadi M, Dastjerdi MB, Ai A, Ahmadi A, Godarzi A, Rahimi A, and Ai J. Horseradish peroxidase-catalyzed hydrogelation for biomedical applications. 2018 Jun. DOI: 10.1039/c8bm00056e

32. Jin R, Moreira Teixeira L, Dijkstra P, van Blitterswijk C, Karperien M, and Feijen J. Enzymatically-crosslinked injectable hydrogels based on biomimetic dextran–hyaluronic acid conjugates for cartilage tissue engineering. Biomaterials 2010; 31:3103–13. DOI: https://doi.org/10.1016/j.biomaterials.2010.01.013. Available from: https://www.sciencedirect.com/science/article/pii/S0142961210000141

33. He C, Ji HF, Qian Y, Wang Q, Liu X, Zhao W, and Zhao C. Heparin-based and heparin-inspired hydrogels: size-effect, gelation and biomedical applications. Journal of Materials Chemistry B 2019 Jan; 7. DOI: 10.1039/C8TB02671H

34. Li X, Xu Q, Johnson M, Wang X, Lyu J, Li Y, McMahon S, Greiser U, A S, and Wang W. A chondroitin sulfate based injectable hydrogel for delivery of stem cells in cartilage regeneration. Biomaterials Science 2021 Jun; 9:4139–48. DOI: 10.1039/D1BM00482D. Available from: https://pubs.rsc.org/en/content/articlehtml/2021/bm/d1bm00482d%20https://pubs.rsc.org/en/content/articlelanding/2021/bm/d1bm00482d

35. Chun YY, Yap ZL, Seet LF, Chan HH, Toh LZ, Chu SWL, Lee YS, Wong TT, and Tan TTY. Positive-charge tuned gelatin hydrogel-siSPARC injectable for siRNA anti-scarring therapy in post glaucoma filtration surgery. Scientific Reports 2021 11:1 2021 Jan; 11:1–14. DOI: 10.1038/s41598-020-80542-4. Available from: https://www.nature.com/articles/s41598-020-80542-4

36. Fu Y, Zoetebier B, Both S, Dijkstra PJ, and Karperien M. Engineering of optimized hydrogel formulations for cartilage repair. Polymers 2021 May; 13:1526. DOI: 10.3390/polym13091526. Available from: https://doi.org/10.3390/polym13091526

37. Wang R, Damanik FFR, and Zhong L. "Macromolecular Paranymphs: Macromolecular Engineering of In-situ Forming Hydrogels. DOI: 10.3990/1.9789036540230

38. Moreira Teixeira LS, Bijl S, Pully VV, Otto C, Jin R, Feijen J, Van Blitterswijk CA, Dijkstra PJ, and Karperien M. Self-attaching and cell-attracting in-situ forming dextran-tyramine conjugates hydrogels for arthroscopic cartilage repair. Biomaterials 2012 Apr; 33:3164–74. DOI: 10.1016/j.biomaterials.2012.01.001

39. Mc Cormack T, O'Keeffe G, Craith BM, and O'Kennedy R. Assessment of the effect of increased fluorophore labelling on the binding ability of an antibody. Analytical Letters 1996; 29:953–68. DOI: 10.1080/00032719608001447

40. Szabó Á, Szendi-Szatmári T, Ujlaky-Nagy L, Rádi I, Vereb G, Szöllősi J, and Nagy P. The Effect of Fluorophore Conjugation on Antibody Affinity and the Photophysical Properties of Dyes. Biophysical Journal 2018; 114:688–700. DOI: https://doi.org/10.1016/j.bpj.2017.12.011. Available from: https://www.sciencedirect.com/science/article/pii/S0006349517350919

41. Lagarto JL, Nickdel MB, Kelly DJ, Price A, Nanchahal J, Dunsby C, French P, and Itoh Y. Autofluorescence Lifetime Reports Cartilage Damage in Osteoarthritis. Scientific Reports 2020 Dec; 10:1–9. DOI: 10.1038/s41598-020-59219-5. Available from: www.nature.com/scientificreports

42. Jung T, Schauer U, Heusser C, Neumann C, and Rieger C. Detection of intracellular cytokines by flow cytometry. Tech. rep. 1993 :197–207

43. Commonly Used Fluorochromes and Their Properties - University of Mississippi Medical Center. Available from: https://www.umc.edu/cancerinstitute/Cancer-Research/Core-Facilities/Flow%20Cytometry%20Core/Resources/Commonly-Used-Fluorochromes-and-Properties.html [Accessed on: 2021 Jul 5]

44. Patil NS, Dordick JS, and Rethwisch DG. Macroporous poly(sucrose acrylate) hydrogel for controlled release of macromolecules. Biomaterials 1996 Dec; 17:2343–50. DOI: 10.1016/S0142-9612(96)00089-0

A APPENDIX

A.1 Washing out free dye

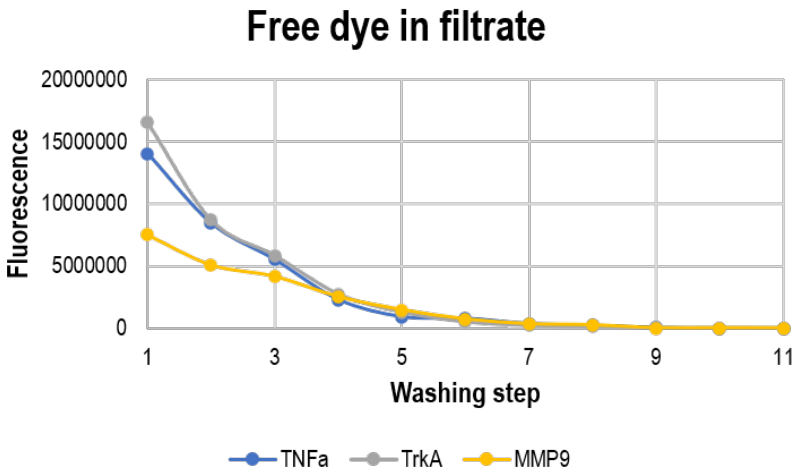

Figure A.1: Fluorescence measurements of each of the collected samples after centrifugation during the washing steps in the labelling process. These measurements show that almost all free dye was washed out of the sample after 11 washing steps.

A.2 Nanodrop measurements

Table A.1: Absorbance measurements of the labelled VHH samples with the Nanodrop at 280 and 495 nm, that were used to calculate the concentration of the labelled VHHs in the samples and to detect the FITC dye respectively.

VHH type	280 nm absorbance	495 nm absorbance
MMP9 unlabelled	0.125	0.003
MMP9 labelled	0.049	0.102
TrkA unlabelled	0.035	0.009
TrkA labelled	0.019	0.016
TNFα unlabelled	0.081	0.021
TNFα labelled	0.059	0.093

Table A.2: An overview of the calculated concentrations of the labelled VHHs, based on the absorbance measurements with the Nanodrop.

VHH type	Stock concentration (µg/mL)	Labelled concentration (µg/mL)
MMP9	850	330
TrkA	1850	990
TNFa	540	390

A.3 BCA assay

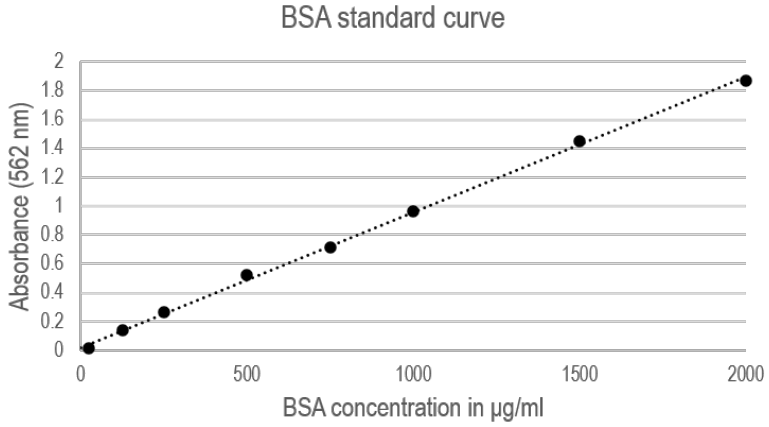

Figure A.2: BSA calibration curve used to determine the concentration of the labelled VHHs.

Table A.3: An overview of the measured absorbance of the VHH samples that was converted to a concentration by using the BSA calibration curve. These concentrations were afterwards scaled to the already known concentrations of the non-labelled VHH samples.

VHH type	Absorbance	Concentration (µg/mL)	Scaled concentration (µg/mL)
MMP9	1.1980	1310	850
MMP9 + FITC	0.3460	364	236
TrkA	1.6931	1860	1850
TrkA + FITC	0.1790	178	177
TNFa	0.9547	1040	540
TNFa + FITC	0.2890	300	156

A.4 Fluorescence measurement after labeling

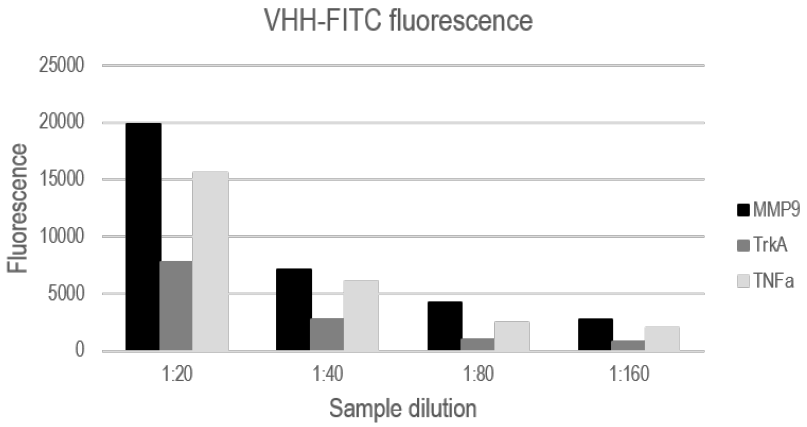

Figure A.3: Fluorescence measurements of serially diluted labelled VHH samples, to show that the labelling process was successful.

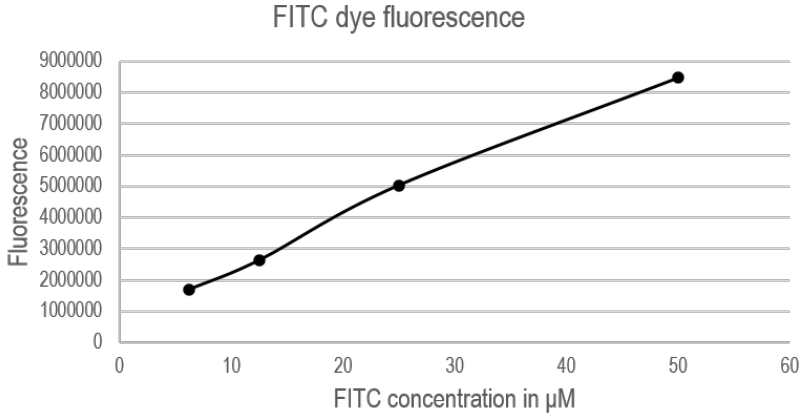

Figure A.4: A fluorescence measurement of free FITC dye in different concentrations, to provide insight into the amount of dye attached to the VHHs.

A.5 Fluorescence intensity of the hydrogels in experiment 1

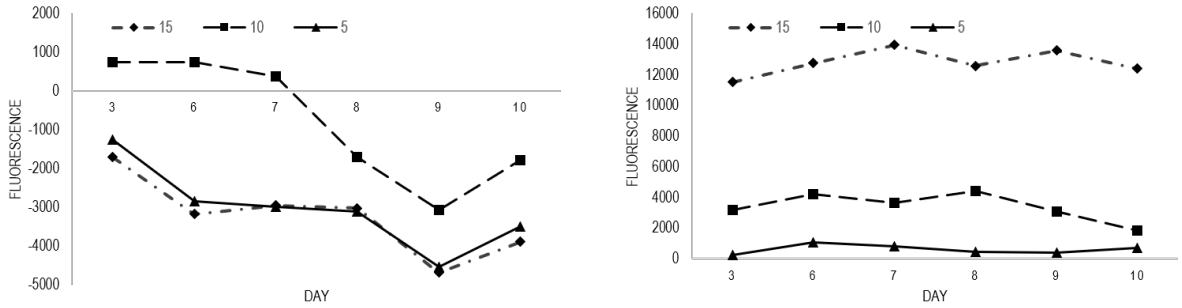

(a) **(b)**

Figure A.5: The fluorescence intensity of the **(a)** HA-TA and **(b)** CS-TA hydrogels themselves with anti-MMP9 VHHs incorporated. These measurements were performed between day 3 and day 10.

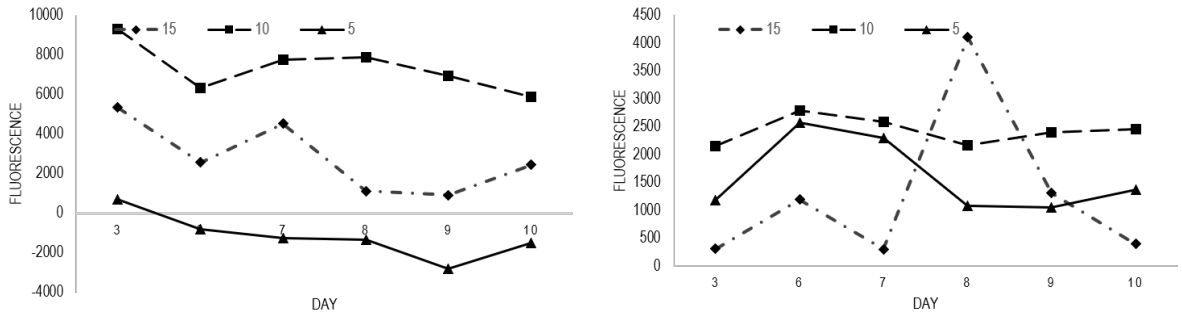

(a) **(b)**

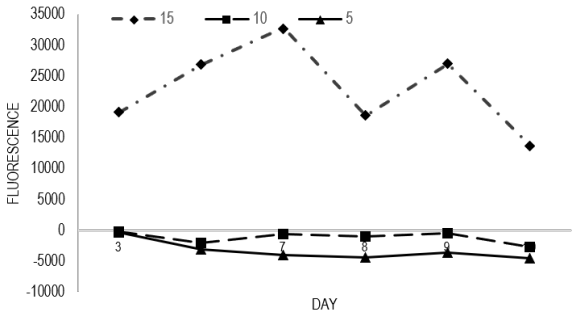

(c)

Figure A.6: The fluorescence intensity of the **(a)** HA-TA, **(b)** CS-TA and **(c)** Dex-TA hydrogels themselves with anti-TNFα VHHs incorporated. These measurements were performed between day 3 and day 10.

A.6 Absolute fluorescence intensity of the hydrogels in experiment 2

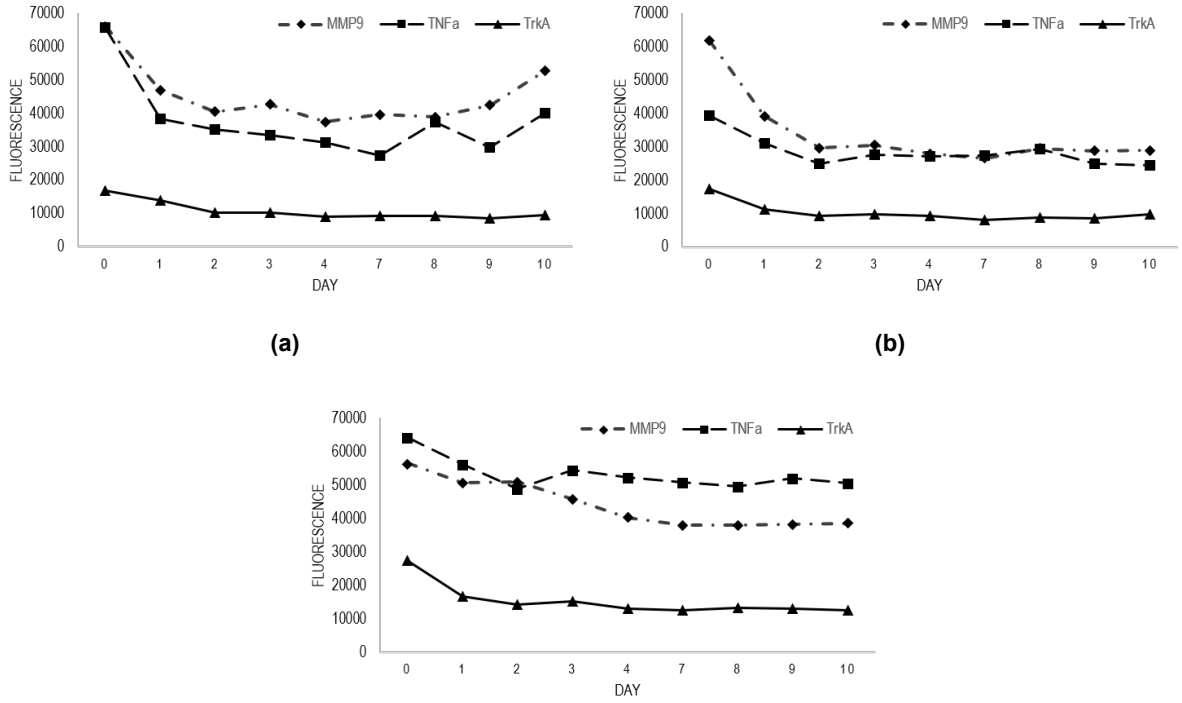

(a) **(b)**

(c)

Figure A.7: The absolute fluorescence intensity of the **(a)** Dex/Gel-TA, **(b)** Dex/Hep-TA and **(c)** Dex-TA hydrogels themselves.

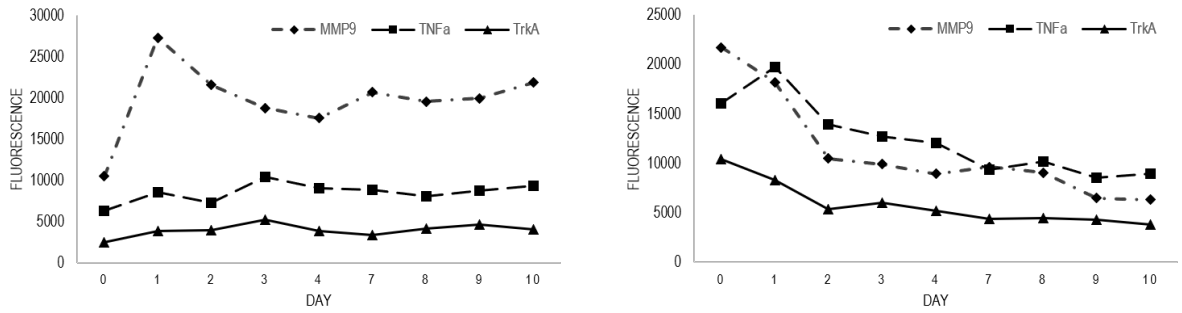

(a) **(b)**

Figure A.8: The absolute fluorescence intensity of the **(a)** HA-TA and **(b)** CS-TA hydrogels themselves.

A.7 ELISA calibration curves

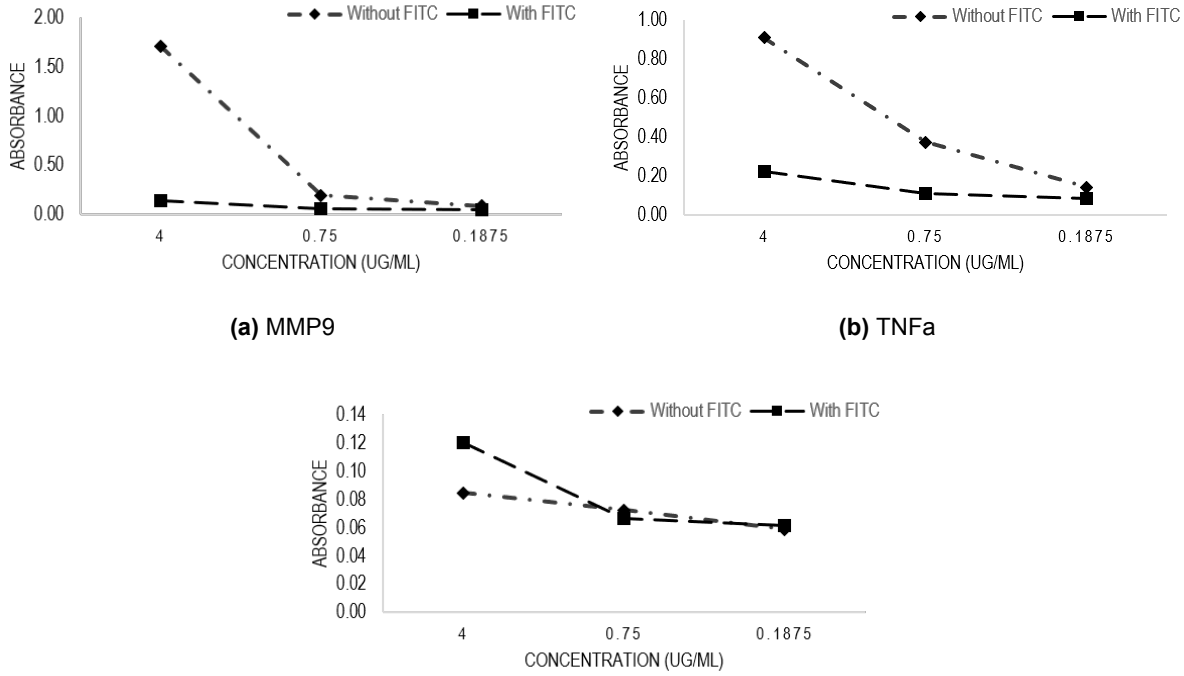

(a) MMP9

(b) TNFa

(c) TrkA

Figure A.9: Calibration curves to provide insight into the VHH concentration in the collected PBS sample used in the ELISA assays.